Atomic-scale nanowires: physical and electronic structure

2004 J. Phys.: Condens. Matter 16 R721

(http://iopscience.iop.org/0953-8984/16/24/R01)

INSTITUTE OF PHYSICS PUBLISHING JOURNAL OF PHYSICS: CONDENSED MATTER

J. Phys.: Condens. Matter **16** (2004) R721–R754 PII: S0953-8984(04)52597-3

TOPICAL REVIEW

Atomic-scale nanowires: physical and electronic structure

D R Bowler[1]

Department of Physics and Astronomy, University College London, Gower Street, London WC1E 6BT, UK
and
London Centre for Nanotechnology, University College London, Gower Street, London WC1E 6BT, UK

E-mail: david.bowler@ucl.ac.uk

Received 13 February 2004
Published 4 June 2004
Online at stacks.iop.org/JPhysCM/16/R721
doi:10.1088/0953-8984/16/24/R01

Abstract

The technology to build and study nanowires with sizes ranging from individual atoms to tens of nanometres has been developing rapidly over the last few years. We survey the motivation behind these developments, and summarize the basics behind quantized conduction. Several of the different experimental techniques and materials systems used in the creation of nanowires are examined, and the range of theoretical methods developed both for examining open systems (especially their conduction properties) and for modelling large systems are considered. We present various noteworthy example results from the field, before concluding with a look at future directions.

(Some figures in this article are in colour only in the electronic version)

Contents

[1] http://www.cmmp.ucl.ac.uk/~drb/

1. Introduction

The ever-shrinking feature size in commercial integrated circuits (at the time of writing, IBM, AMD and Intel are starting to produce chips in volume from 0.09 μm, or 90 nm, fabrication lines) combined with the ability to manipulate atoms and molecules with increasing precision is driving a huge research effort into alternatives to the conventional, lithography-based fabrication of semiconductor devices. Self-assembly, *ex situ* assembly and *in situ* fabrication by scanning probes are all techniques being used to create novel structures. At the same time, theoretical methods to address accurately both large systems and open systems (and hence their conduction properties) have been developed. This paper concentrates very specifically on nanowires, focusing on semiconductor substrates and the atomic-scale end of this broad subject, and covers both the practical applications towards nanoelectronics and the fundamental science involved in creating and studying these systems.

There are many reasons for studying nanoscale wires. First, conduction properties in one-dimensional systems are different to those in two- or three-dimensional systems, giving rise to phenomena such as quantized steps of conductance [1], Peierls distortions and charge density waves [2] and Luttinger liquid behaviour [3–5]. The ability to measure the conduction and physical properties of systems displaying these phenomena has immeasurably improved our understanding of conduction in restricted structures, though (as will become clear) there are still major questions remaining open. Second, alternatives to electron beam lithography need to be investigated. While recent work has shown that the limit of feature size can be taken below 20 nm [6, 7] (even as low as 5 nm [8]), the resulting wires are inevitably polycrystalline, and subject to failure at rather low current densities [9]. The use of nanowires from self-assembly, deposition or *in situ* fabrication to replace these wires is a subject of intense research. Practical applications of nanowires and molecules for nanoelectronics have been demonstrated, including functioning logic elements [10–14], memory [11] and switches [15], which while not of any immediate technological application show that the field is active and that the potential exists for useful end results. We also note that emerging fields such as the search for solid-state quantum computing elements will require the ability to address individual atoms or molecules, and hence interconnects on a scale of a few nanometres.

This is a *topical* review, and will hence be rather limited in scope and choice of systems (in part to the areas of the author's interest!). In particular, it is worth emphasizing that the only substrates being considered are semiconductors or insulators: there is not space, or time, to consider the work on metal substrates (or the fascinating field of superconducting leads and nanowires). There have, of course, been other recent reviews which cover similar or related ground to this paper: on transport in nanowires [16] (which concentrates rather more on thermal transport and carbon nanotubes); on carbon nanotubes [4, 17]; on nanomaterials (including surfaces) [18]; on quantum properties of atomic-size conductors [1]; on molecular conduction [19, 20]; on scanned probe microscopy of single molecules [21, 22]; on scanned probe techniques (often used to characterize the structure and transport properties of these wires) in general [23]; on conducting polymers and carbon nanotubes [24]; and on magnetic nanostructures (which has relevant material on growth of wires and properties of one-dimensional structures) [25]; this last topic is described further (with more references to relevant reviews) in section 4.4, which deals with spin transport. There is an older review on electromigration in metals [26] which sets the scene for many of the technological problems facing makers of integrated circuits.

1.1. Quantum of conductance

The quantum of conductance for a one-dimensional metallic channel is now well established as $2e^2/h$, as predicted by Landauer [27]. One way of arriving at this formula is as follows [16, 28]. We start with the Drude formula for conductivity,

$$\sigma = \frac{ne^2\tau_m}{m^\star}, \tag{1}$$

where $m^\star$ is the effective mass, n is the density of electrons and τ_m describes the characteristic relaxation time between collisions for the charge carriers. Now for a one-dimensional conductor with a single metallic channel (the simplest possible system that we can consider) the density tends to $n = 2k_F/\pi$ for the Fermi wavevector k_F. For a sample of length L we find that the conductance is

$$\begin{aligned} G = \frac{\sigma}{L} &= \frac{2k_F e^2}{\pi L m^\star}\tau_m = \frac{2e^2}{h}\left(\frac{2\hbar k_F}{Lm^\star}\tau_m\right) \\ &= \frac{2e^2}{h}T\left(=\frac{e^2}{\pi\hbar}T\right). \end{aligned} \tag{2}$$

Here, we have identified a transmission coefficient, $T = (\frac{2\hbar k_F}{Lm^\star}\tau_m) = 2v_F\tau_m/L$, with v_F the Fermi velocity. As the transmission coefficient approaches 1, the conductance approaches the fundamental quantum of conductance (which is equal to $(12.9\ \mathrm{k}\Omega)^{-1}$). This conductance is for a single channel; when considering real systems, the number of channels open at a given bias has to be considered and summed over.

There have been various investigations into the nature of this conductance, mainly concentrating on extremely narrow, ultimately single-atom, wires. Most of these experiments are detailed in section 2.1, but the key conclusion is that for certain systems (particularly monatomic gold wires), steps of conductance equivalent to a single quantum can be observed.

1.2. What is a nanowire?

Over the last few years, the prefix 'nano' has become extremely popular, partly through its ability to attract funding, but mainly through the development and refinement of techniques such as scanning probe microscopies and density functional theory which allow experimental

construction and observation and theoretical modelling of structures on the nanoscale. However, it tends to be applied somewhat indiscriminately to any system which has at least one dimension below 1 μm.

In this review, we are interested in systems which are confined to a *few nanometres* in *two dimensions*, or at most to a few tens of nanometres. To meet the criterion of wire, some degree of elongation in the third dimension is important. This describes the physical (or geometrical) constraints considered. The use of the term 'nanowire' is often applied without reference to conduction properties of the system, and simply describes nanolines or (possibly) nanowhiskers: long, thin nanoscale systems. The systems considered in this review will, generally, be conducting or semiconducting (with a small enough gap to have interesting properties), or be related to possible conducting systems.

The rest of the review is organized as follows. First, various experimental realizations of nanowires are considered, concentrating on atomic-scale systems, and biased towards the Si(001) surface as a substrate (mainly because of its technological importance). The following section considers theoretical approaches to modelling the electronic structure and conduction properties of these systems. Some of the important and interesting results from the field are then highlighted, whenever possible drawing theory and experiment together (though one thing that will become clear from this section is the disparity between the two disciplines). The review then concludes by looking at possible future directions for the field.

2. Experimental realization

In this section, various techniques for preparing nanowires, and systems which form nanowires, are presented. A selection of recent interesting results, both experimental and theoretical, based on these systems will be presented in section 4. We start with atomic-scale contacts (as epitomized by the mechanically-controllable break junction), move on to hydrogen masking on Si(001) (and the structures that can be formed by removing the hydrogen and adding material), followed by self-assembled wires on Si(001) (in particular the structures formed by rare-earth wires), then finishing with systems which are formed *ex situ* and are deposited on substrates: organic semiconductors, carbon nanotubes and semiconductor nanowires.

2.1. Quantized conductance in atomic-scale contacts

The archetypal system for studying one-dimensional conduction, conductance quantization and atomic-scale wires is the atomic-scale contact: formed from a mechanically-controllable break junction (MCBJ), an STM tip 'dipped' into a metal surface and withdrawn (and other methods, including 'table tapping'), these contacts are gradually thinned until they are a single atom wide. There has been an extraordinarily thorough review on this subject published recently [1] to which the interested reader is strongly directed; we will only highlight a few interesting and relevant results here.

Early measurements involving contact between gold surfaces and STM tips [29] found that as the substance joining the STM and the surface was stretched, the current became quantized (reflecting the quantum of conductance discussed above). These results were repeated [30] and also observed in a different, simpler technique: macroscopic wires that were induced to jump in and out of contact by tapping the table the experiment was situated on [31]. More sophisticated measurements have concentrated on identifying the number of channels open in different materials by measuring shot noise as well as current [32], and find that gold (which proves to be a special example) has only one channel, but other materials, such as aluminium, have a number of different channels. Measurements can also be carried out at high bias [33, 34],

which shows that this reduces the lifetime of the conduction peaks, and a possibility of washing out the quantization (which could well be due to atomic rearrangements, as discussed below).

With gold as the system to be studied, a single chain of atoms with a single conductance quantum can often be achieved with care. The structure of the chain of atoms is rather controversial, however. It has become possible to image such chains in a transmission electron microscope (TEM) [35], though the unequivocal assignment of positions and spacing is still debated. The observed spacing of ∼3.5 Å from TEM [35] contrasts with ∼2.5 Å, that was observed (or inferred) from conductance histograms [36], and with the bulk nearest-neighbour distance. This issue will be discussed fully in section 4.1.

Modelling of these systems has tended to concentrate on either the mechanical properties of the system (using empirical potentials, tight binding or full *ab initio* simulations) or conductance of the system (using tight binding or *ab initio* simulations); many of the *ab initio* codes represented the electrodes as jellium (with one or two layers of atoms on top to allow correct interactions). Only recently have *ab initio* methods appeared which treat the atomic structure of the device and electrodes [37, 38], though the level of importance of this detailed treatment is not clear; it is often enough to include the top layer or two of atoms in the electrodes as part of the device and replace the rest of the electrode with jellium.

Work on electronic structure has included zero-bias and finite-bias calculations, with levels of approximation from tight binding to *ab initio*. The systems considered are metallic, and cover many systems. Example common materials include: Al [39–46]; Na [39–41, 47, 48]; Au [30, 37, 44, 46, 49–51] and others, such as Pb [44] and Nb [45]. Gold, which is used rather frequently in these experiments and calculations, has been found to be unusual: much of the electronic structure comes from the 6s orbitals, leading to a single conductance channel which is almost completely open under most circumstances. This gives rise to the well-defined conductance plateaus, where other metals, which have a more complex electronic structure and hence more conductance channels with variable and easily affected coefficients, display less clear behaviour.

2.2. H masking of Si(001)

The Si(001) surface is technologically the most important surface of silicon, as this is where all devices are grown. The surface itself reconstructs, with atoms pairing up to form dimers, which align in rows along the (110) directions. These dimers buckle (in a Jahn–Teller distortion) with the sense of the buckling typically alternating along the dimer row. This yields the p(2 × 2) and c(4 × 2) reconstructions often seen at low temperature in the STM. However, at room temperature, the dimers flip back and forth between the two senses, yielding a flat appearance in the STM. These features are all illustrated in figure 1(a). There are three terraces visible; in the lowest, at the bottom left, dimer rows run diagonally from upper left to bottom right. In subsequent terraces, the dimer direction rotates by 90° at each step because of the underlying crystal structure. The buckling of the dimers can be seen 'frozen' at a step edge in the top right of the image; this phenomenon is a result of an increased barrier to flipping at the step edge.

The dimers themselves are extremely reactive, having one dangling bond per atom, but can be easily passivated by atomic hydrogen to yield a monohydride surface. Various experiments have now shown that it is possible (via what might be called nanolithography) to define wires one atom wide on this surface by the selective removal of hydrogen atoms [52–55]. Starting with a hydrogen passivated surface, the STM tip is used to apply a voltage pulse which can desorb individual hydrogen atoms from the surface [54, 56], leaving behind a dangling bond (DB: an unpaired electron on a surface atom). This can be used in two different ways: either

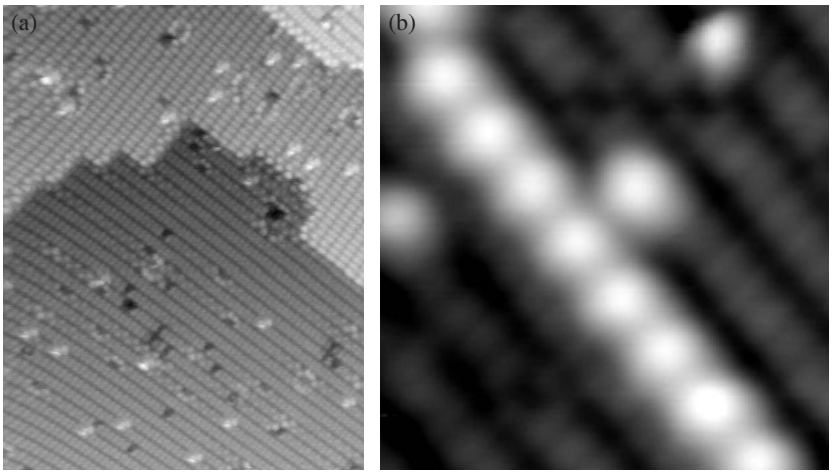

Figure 1. (a) STM image of a Si(001) surface, 24 nm by 32 nm. Note the dimer rows running diagonally across the image in the (110) directions. The buckling of dimers is often frozen at step edges (for instance in the top right) appearing as a zig-zag pattern. *Image courtesy of Tetsuya Narushima.* (b) A dangling bond wire (bright spots) running along a dimer row on hydrogen-terminated Si(001). Alternate atoms are up (visible as large, white protrusion) and down (not visible). The hydrogenated dimers, running from top left to bottom right, appear much darker. *Image courtesy of Taro Hitosugi.*

to create a line of dangling bonds (a dangling bond wire) or as a nanoscale pattern for later adsorption of metals or gases.

If the dangling bond wire runs along the underlying dimer rows, then the resulting metallic structure undergoes a Peierls distortion to form a semiconducting line of dangling bonds, which alternate in height along the wire [57]. An example of a DB wire running along a dimer row can be seen in figure 1(b). Only the higher atoms can be seen (due to their increased charge as much as height), with the lower atoms lying between the bright dots. The electronic structure of the wire shows a finite density of states (DOS) at the Fermi level in scanning tunnelling spectroscopy (STS) [55]. Short, odd length wires have been suggested recently to show little physical buckling, but strong spin polarization along the wire, with up and down spins alternating in place of the up and down atoms [58]; the physical displacements are in good agreement with STM measurements [57], but there is no measurement of the electronic structure. Details of modelling work on the effect of injecting charge into these systems will be given in section 4.5.

As an alternative to the bare silicon used in DB wires, materials can be adsorbed onto the exposed silicon which is, in general, more reactive than the hydrogenated surface. This is equivalent to the use of hydrogen as a mask on the nanoscale. (We note that this is not always suitable; for instance, Si or Ge will adsorb *under* the hydrogen, which is used as a surfactant during growth.) Adsorbates considered include oxygen [52, 53], iron [59], gallium [60, 61], aluminium [62], cobalt [63], silver [64, 65] and organic molecules such as norbornadiene [66–68]. The adsorption of metals generally results in a high concentration of metal clusters on the depassivated areas, with wire-like structures forming with increasing metal deposition. The resulting structures are rather poor though, with variable width and many imperfections. There are also small clusters of metal on the hydrogenated surface. The experiments with organic molecules found that the depassivated areas acted as binding sites for the molecules, leading to predefined arrays of the molecules on the surface.

The adsorption of Ga [61, 69, 70] and As [71] on DB wires has been modelled from first principles, as has the doping of bare DB wires with Na [72]. As might be expected, the electronic structure of the resulting wires depends rather strongly on the adsorbate positions and bonding. The resulting wires tended to show flat bands near the Fermi level, though K doping of the As wires [71] suggested that a ferromagnetic wire might be possible. The Na doping of wide DB wires (where an entire dimer row is depassivated) found that a metallic wire resulted.

A different approach found a chain reaction which was initiated by the desorption of a *single* hydrogen atom [73]. A small amount of styrene was admitted to the UHV chamber, and a single dangling bond created on a hydrogenated Si(001) surface with the STM tip. A styrene molecule reacted with the dangling bond, adsorbing onto the silicon. After adsorption, the molecule then reacted with an *adjacent* hydrogen atom on the surface, abstracting it and leading to another dangling bond. This led to a chain reaction, and the formation of lines of styrene molecules on the hydrogenated surface.

2.3. Self-assembled wires and lines on Si(001)

Self-assembly is attractive as it is not labour-intensive: allowing wires or devices to form on a surface requires little or no human intervention. However, it has the drawback that there is much less control over the location of the wires which form. (The self-directed growth of styrene wires [73] mentioned above is an interesting compromise between these two approaches.)

One class of metals which are extremely interesting from this point of view are various of the rare-earth metals. When one of these materials is deposited on Si(001) and annealed, it forms compounds XSi_2 in the AlB_2 structure with the *c* axis perpendicular to the surface; parallel to the Si(001) surface, this tends to match the silicon lattice constant in one direction but very poorly in the other, leading to the formation of long, straight wires due to the effects of strain. This was first observed for Dy [74–78], and later for Er [76, 79], Ho [75, 80], Gd (and, though not a rare-earth metal, Sc) [76, 81]; it is interesting to note that Nd, Sm and Yb do not form wires, but compact islands [75]. These wires tend to be a few nanometres wide (1.5–10 nm) and grow up to several microns long. Measurements via STS show that these wires are metallic [80, 81]. The wires are straight, but their structure is often defective; they will not cross steps, and grow out from a step edge, forming a promontory of Si around them [75, 78, 80]. Attempts to use this technique for $TiSi_2$ [82] have found that the results are rather poor: the Ti tends to diffuse into the bulk. Growth of nickel silicide wires by the reaction of silane (SiH_4) with nickel thin films on SiO_2 results in the formation of wires of diameters around 15 nm, though this depends on the growth temperature [83]. Large-scale $CoSi_2$ wires (with widths of $\sim$70 nm) form on the surface after annealing of a silicon substrate with Co implanted subsurface [84], though these are rather larger than most wires considered in this review.

Another class of self-assembled line (rather than wire) is the Bi nanoline [85], which forms spontaneously when a Bi-covered Si(001) surface is annealed at between 570 and 600 °C. This temperature window is important: too low, and the lines do not form; too high, and the lines desorb. The defining characteristics of the lines are their perfection and length: they are always 1.5 nm wide (equivalent to four substrate dimers), often exceed several hundred nanometres in length, and are never kinked or defective [86]. An image of these lines forming in a disordered, Bi-covered surface is shown in figure 2(a). The lines grow out from down step edges (relative to the terrace in which they are growing) and 'tunnel into' up step edges, as clearly seen in the figure. As with the rare-earth silicides, these lines seem to form due to strain, though their electronic structure [87] shows that they are, in fact, semiconducting with a larger band

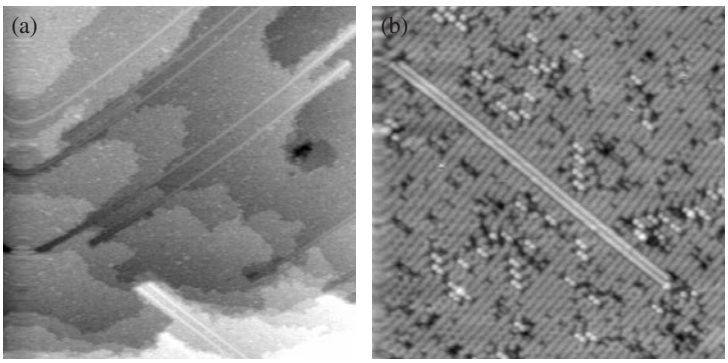

Figure 2. (a) A large-scale STM image of Bi nanolines on Si(001), 160 nm × 160 nm. Note that the lines are perfectly straight, and run across the entire image. The image was taken at high temperature, while Bi is still present on the surface. (b) An STM image of the Bi nanoline, 40 nm × 40 nm. The double structure of the lines can clearly be seen, along with their location relative to the underlying substrate. *Images courtesy of James Owen*.

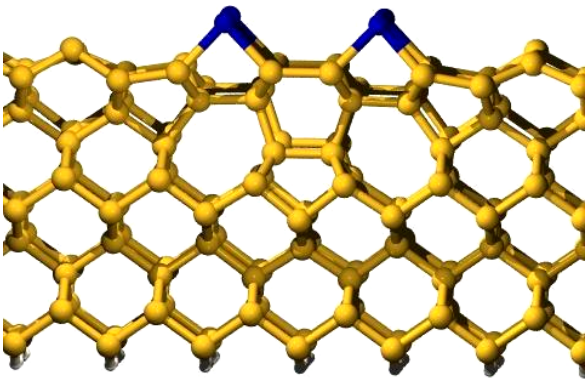

Figure 3. The structure for the Bi nanolines. Note the significant subsurface reconstruction, characterized by five- and seven-membered rings. The silicon atoms are lighter, and the bismuth atoms (two dimers) darker.

gap than the surrounding silicon, so to be used as wires they would need either doping or overgrowth.

A detailed STM image of the Bi nanoline is shown in figure 2(b). The doubled nature of the nanoline, consisting of pairs of dimer-like features, is clear. Detailed measurements found that these double features lie *between* the dimers of a dimer row in the underlying Si(001) surface, but on top of the dimer row [88]. The atomic structure of the Bi nanoline is shown in figure 3. The structure was deduced based on STM images, growth data, XPD and PES data and extensive electronic structure modelling [85]. The key point to note is the reconstruction of the substrate beneath the Bi dimers, featuring five- and seven-membered rings (leading to the unofficial name of 'Haiku', by analogy with the Japanese poetry form consisting of lines with five, seven and five syllables). This reconstruction explains the extraordinary straightness of the lines, as the kinking energy is over 2 eV. It seems to be a compromise between relieving strain associated with the long Bi–Si and Bi–Bi bonds and straining the surrounding silicon, as seen in detailed STM imaging and electronic structure modelling [87]. As with the rare-earth silicides, the growth is associated with lattice matching in one direction (perpendicular to the dimer rows) but not in the other.

When Ga, In or Pb are deposited on Si(001) at room temperature and low coverages (∼0.1 ML), they form long, one-dimensional chains [89, 90]. These chains run perpendicular to the underlying dimer rows, and consist of metal dimers located over the trenches between the dimer rows. Some work has been done on understanding the growth mode of these lines, and limited work on their conduction properties (STS finds that, for perpendicular tunnelling, there is a substantial band gap [90]), but there has not been any work on how they might be used or isolated from the surrounding silicon.

These structures have been refined, by using an underlying reconstruction of Si(001). If a small amount of Ni is added to the Si(001) surface, semi-ordered lines of missing dimer defects form, similar to those seen during sub-monolayer growth of Ge on Si(001). These dimer vacancy lines (DVLs) yield a $(2 \times n)$ reconstruction. Adding In [91] or Ga [92] to this surface results in long-range ordered wires of the metal. This technique had been used earlier, in reverse, to form Fe wires on Si(001) [93]: after forming the Ni-induced $(2 \times n)$ reconstruction, the surface was masked by water adsorption, and Fe evaporated from a solid source. It was found that the Fe formed nanolines which nucleated in the DVLs, rather than on the Si(001) surface; the quality of these lines is a little poorer than the equivalent Fe wires deposited on DB wires [59], but the lines were spread across the entire surface. Very recently, the reconstructed surface resulting from deposition of 1 ML of Ge on Si(001) surface has been used to form ordered lines of styrene, confined between the dimer vacancy lines [94].

Steps and step edges can be used to form arrays of wires: on Si(001), arrays of Ge wires can be formed [95], and similar wires form on Si(113) [96]. Using Bi as a surfactant, Ge nanowires can be grown at step edges of Si(111), resulting in wires 3.5 nm wide and 0.3 nm thick [97]; two-dimensional growth using the same technique results in nanorings, and, by growing Ge and Si successively, a superlattice of Ge and Si nanowires can be formed at the surface. $GdSi_2$ wires can be formed on Si(111) [98], and attach to step edges exclusively. There are many other interesting classes of step arrays and wires based on these arrays on the Si(111) surface. By miscutting a sample towards (112)-like directions, regular arrays of steps are formed with extremely low kink densities [99]. There has been much recent work on noble metals on Si(111) and related vicinal surfaces (in particular Si(557)) where chains of Au and Ag atoms are formed [100–104]. Early measurements suggested that these chains might be Luttinger liquids [105], though more recent studies suggest that this is not the case [103, 106]. Other interesting effects can be observed on this surface: the In(4×1) reconstruction on Si(111) has yielded a plausible observation of a Peierls distortion directly in STM [2]; and Na on Si(111) chains seem to show Mott–Hubbard insulator properties [107].

2.4. Organic molecules

One large area of research in atomic-scale wires is, of course, organic molecules. The field is extremely large, encompassing both bulk-like (and thin film) samples and transport through single molecules (which is more relevant to this review). A particularly relevant review on the transport properties of conducting polymers (and carbon nanotubes, which appear below in a separate section) has been published recently [24]. While this is an enormous field, one result on conduction in bulk-like samples is particularly interesting: the conductivity is limited ultimately by the chain–chain hopping: a class of polymer called regio-regular polymers which align and give good inter-chain contact has been found to be important in improving this hopping [108, 109].

The transport characteristics of single molecules are generally studied through some form of metal–molecule–metal junction (formed by deposition between lithographically defined electrodes on a surface [110], by self-assembly into a monolayer in a pore and overgrowth

of gold [111] or by insertion into a self-assembled monolayer of inert molecules on a gold substrate and subsequent contacting with a gold-plated AFM probe [112]). The molecules used in these junctions are often well characterized in their atomic and electronic structure, since they have been chosen and (in some cases) designed for specific properties. However, the effects of electric field, assembly into a monolayer, bonding to a surface and other processing steps can have a large effect on both of these areas. An excellent recent review of scanned probe studies of single molecules covers several of these effects [21].

One area of intense, and controversial, effort recently has been that of single molecule conduction, starting with the experiment of Reed *et al* [113] which involved measuring the conductance of a self-assembled monolayer (SAM) of benzene-1,4-dithiolate via an MCBJ. There have been further attempts to make current measurements reproducible involving inserting dithiol molecules into SAMs of alkane thiols on Au [112] and measurements of switching in similar systems [114–116]. A recent paper has concentrated on statistical data, measuring the conductance of thousands of junctions [117]. While it is impossible to generalize, the $I(V)$ characteristics of such molecules often show a gap, and are capable of carrying currents up to a few tens of microamperes.

A major issue in interpreting these results is the quality and reliability of the junction between the molecule and the electrodes. It has been shown for H_2 and Pt electrodes [118] that it is possible to achieve excellent coupling to electrodes for a single molecule, and achieve the theoretical value (conductance of $0.9G_0$) expected for the molecule. Another technique for forming reliable junctions involves a lithographically defined, nanometre-scale wire which is broken by electromigration [119], while surrounded by a solution containing the molecule of interest [110]; this results in a junction bridged (potentially) by single molecules. This technique has recently been used to measure the Kondo resonance in molecules containing vanadium [120] and cobalt [121]. A final technique involves the sequential deposition of source, a self-assembled monolayer of the candidate molecule and drain on a quartz tip [122].

Modelling of these devices has used techniques to be described in detail in section 3, using methods ranging from tight binding to full *ab initio*. The results will be presented in section 4.2. It is worth mentioning here an extensive study of the bonding of different molecules to gold [123], whose major conclusion is that the geometry of the bonding is of paramount importance.

One fascinating recent development, the effects of which have yet to be tested on electronic structure at the single molecule scale, is the 'insulation' of polymer chains by encapsulation in cyclodextrin [124]. Cyclodextrin is a cyclic molecule consisting of a number of glucose molecules (between 6 and 8) which form a ring. The structure is roughly cylindrical, with an interior diameter between 0.45 and 0.85 nm [125]. The interior of the ring is hydrophobic, while the exterior is hydrophilic, providing one mechanism for encapsulation of polymers. AFM measurements suggest that the polymer becomes completely encapsulated within a sheath of cyclodextrin molecules (which can be cross-linked to form a single tube) [125]. The beneficial effects in one particular field have been recently demonstrated by measuring the luminescence in solid-state LED-type devices [126].

2.5. Carbon nanotubes

Carbon nanotubes (CNTs), which appear in semiconducting and metallic forms, offer a tantalizing opportunity for robust, *ex situ* fabricated atomic-scale wires. However, there is as yet no way to separate these different forms, which presents a challenging barrier to their adoption as wires. It is worth noting that there have been a number of ingenious suggestions [127–130] which might be better described as routes to enrichment; it has also been shown to

be possible to selectively 'burn out' metallic tubes in air with high current densities, leaving only semiconducting NTs [131]. There have been a number of recent reviews focusing on CNTs [4, 16, 17, 24].

Metallic nanotubes offer possibly the purest example of a one-dimensional conductor, and various effects which differ radically from normal two- and three-dimension conduction (well described by Fermi liquid theory) are expected to be seen. They behave well as quantum wires, showing discrete states which are coherent over the length of the wire [132]. Measurements of the conductance of metallic tubes cooled below 100 K as a function of temperature and voltage show behaviour consistent with tunnelling into a Luttinger liquid, both tunnelling directly into the tubes from electrodes [5] and tunnelling between nanotubes after manipulation to form junctions and crossings [3, 133, 134]. This behaviour arises in one dimension largely from the effects of Coulomb interactions, as predicted theoretically [135, 136]. A recent measurement of the photoemission spectrum of metallic single-walled nanotubes has shown direct evidence of Luttinger liquid properties in the electronic structure [137], adding significant weight to the evidence that the observed behaviour is actually due to a Luttinger liquid.

At lower temperatures (i.e. below about 10 K) the charging energy of the tube between contacts becomes larger than the thermal energy of the electrons, and Coulomb blockade effects can be observed, leading to a complete failure of conductance as the temperature drops to zero [4, 5, 134]. This has been studied in more detail without regard for possible Luttinger behaviour, and peaks in the conductance are observed, which are interpreted as single-electron charging of the nanotube [138]. The high-field transport characteristics suggest that these tubes are capable of supporting current densities of the order of 10^9 A cm^{-2}, though at high bias voltages the conductance drops rather dramatically [139]. There have also been recent reports of measurements of the potential and conductance along nanotubes using scanned-probe techniques [140, 141].

As well as the almost ubiquitous technique of *ex situ* preparation and deposition (normally by spin coating, though there has been a recent report of a dry deposition technique, leading to UHV STM imaging of SWNTs on H–Si(001) [142]), there have recently been efforts to grow nanotubes *in situ* [143–145]. The substrate is pre-patterned with catalytic islands (typically Ni) and growth proceeds via CVD using methane as the gas source of carbon. This technique has been used to build field-effect transistors [143], and recent developments are looking at ways to align the nanotubes so grown [144, 145]. CVD growth of nanotubes is being used to produce SPM tips made from CNTs [146]. Research is also proceeding into the effects of functionalization [145, 147]; it has been found that different types of CNT will react with different reagents (so that, for instance, metallic nanotubes can be functionalized almost exclusively within a sample).

2.6. Semiconductor nanowires

One way around the semiconducting/metallic selection problem inherent in carbon nanotubes is to grow nanowires with the desired properties, and this is what is done with semiconductor nanowires (NWs). While the structures are rather larger than many others considered in this review so far (with diameters typically from 5 to 40 nm, and lengths up to several tens of microns), the results are sufficiently interesting and elegant that they need to be included. The growth technique is based on the vapour–liquid–solid (VLS) technique [148]; a catalytic particle (often gold) acts as the growth site. Growth of the solid nanowire proceeds from the liquid catalyst using a gas-source (vapour) growth medium, which typically forms a eutectic mixture with the catalyst. The method produces single-crystal wires, but the key limitation on the diameter of the wire comes from the size of the catalytic particles. Extensive early

work on GaAs and InAs has been thoroughly reviewed [149]. A key development in growing narrow NWs was the use of laser ablation to create catalytic particles with diameters of a few nanometres [150]. An alternative preparation route involves simple laser ablation of a target of mixed Si and SiO_2 [151]. Use of NWs in logic circuits will be discussed in section 4.3, and deposition and alignment of the wires will be discussed in section 4.6.

Growth of nanowires of various different semiconductors has been demonstrated: Si, Ge and Si/Ge [150, 152–159]; GaAs [156]; GaN [160]; InP [156, 161, 162]; CdS [163]; ZnSe and CdSe [164]. The resulting wires are single crystals [150], though they often have an oxide sheath around the single crystal core. They can be grown in contact with CNTs [157] by using a common catalyst for the growth of the CNT and the NW (the CNT so grown is a multi-walled, metallic tube). Better growth was observed using an Au catalyst and growing the NW on the CNT. Doping of InP nanowires has been demonstrated [162], using Te as an n-type dopant and Zn as a p-type dopant. Heterostructures [154, 155, 161] and, by extension, superlattice wires [154, 156, 164] can be grown. An example of a superlattice is shown in figure 4. This is an InAs/InP superlattice, which clearly shows the crystallinity of the nanowire and the strain around the interfaces between different materials. Detailed TEM 'elemental mapping' of a GaAs/GaP heterostructure [156] showed that the interface was well-localized; the change from GaAs to GaP took place over ∼15 nm, which is equivalent to the diameter of the catalytic particle. This suggests that the time taken to change growth material is simply limited by the time for the eutectic with the catalytic particle to change.

A variation of the heterostructure technique is the core–shell nanowire heterostructure [155]. Here, after growth of a nanowire using the standard technique, the growth conditions are altered so that, instead of growing axially (increasing the length of the wire), the wire grows radially, with nucleation occurring on the surface of the nanowire, not at the catalytic particle. Both homoepitaxy and heteroepitaxy have been demonstrated (Si/Si and Ge/Si) using this technique. This offers interesting possibilities for passivation of surface and electron and photon confinement at least.

Ohmic contacts to the nanowires show that the intrinsic $I(V)$ curves are linear, and that gating effects are clearly visible for doped NWs. (Similar Si nanowires, formed by e-beam lithography, show quantum interference effects when their transport is measured [165].) The surface properties of Si NWs have been investigated [153] by growing Si NWs from SiO, yielding an oxide-coated NW. On stripping the oxide with HF, H-terminated wires with diameters from 1.3 to 7 nm are found, with band gaps (measured from STM and STS) varying from 3.5 to 1.1 eV. The surfaces, as imaged in STM, appear to have (111) and (001) facets. The electronic structure of silicon NWs has been studied with photoemission spectroscopy (PES) and x-ray absorption fine structure (XAFS) [166]. These measurements confirm that the NWs are made from crystalline Si, and that an increasing band gap correlates with decreasing NW diameter; there is a connection with porous Si (which is an effective limit of the NWs). There has been some modelling relevant to this system: *ab initio* calculations of H-terminated rectangular, infinite NWs ranging from 1.2 to 2.3 nm in thickness, which confirmed the correlation between bandgap and NW size (the study also found that effective mass theory can be reliably used for large diameter NWs). A more recent quantum Monte Carlo (QMC) study of nanoclusters with a hydrogen termination suggested that surface reconstruction and steps might be responsible for reduced optical gaps and exciton lifetimes in these systems [167].

There are, of course, other systems that form long, thin structures, though these may not be as robust, conducting or easily processed as earlier systems described: BN nanotubes [168], belts of semiconducting oxides [169], ZnO nanowires [170, 171], MoS_2 nanotubes [172], GaN nanotubes, grown around ZnO nanowires [173] and various rare-earth oxide nanotubes [174].

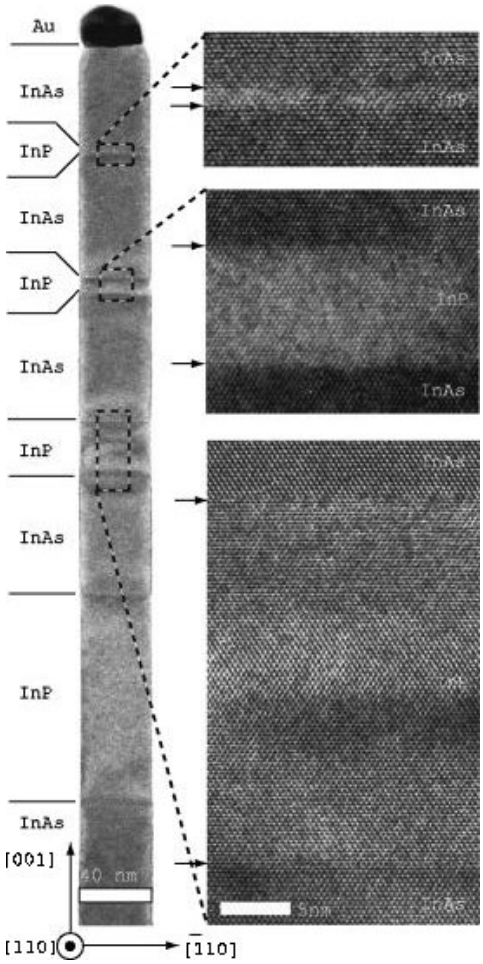

Figure 4. TEM image of an InAs whisker, 40 nm in diameter, containing four sequential InP barriers. The strain fields around each interface can be seen as elliptical, darker areas, having an extension of about 20 nm. In the thickest barrier the crystal is therefore completely relaxed. The magnified views prove that abruptness of the interfaces on the atomic scale is obtained. The figure, from [161], is copyright AIP, reproduced with permission.

3. Theoretical techniques

There are two aspects to the modelling of nanowires: first, the atomic and electronic structure; and second, the conduction properties of the wire itself (which depend, in some cases crucially, on the first aspect). The principles behind modern electronic structure calculations are well established and rather standard, and have been well reviewed elsewhere. The relevant techniques include tight binding [175] and density functional theory [176]. We provide a brief summary for convenience and to highlight points of interest.

3.1. Atomic and electronic structure

All modern electronic structure techniques rely on various approximations. First, they generally work with periodic boundary conditions and invoke Bloch's theorem for periodic wavefunctions. Second, they use the Born–Oppenheimer approximation, which asserts that as

the electrons are so much lighter than the ions we can separate the electronic and ionic degrees of freedom: the ionic forces are calculated for the ground-state electrons using the Hellmann–Feynman theorem, the ions are moved appropriately (either to relax towards a minimum energy configuration or to perform molecular dynamics) and the electronic states re-calculated for the new positions. Finally, some approximation is invoked to transform the inherently many-body problem involving all the electrons in the system into a set of independent electron problems. At this stage, the problem to be solved is essentially the time-independent Schrödinger equation:

$$\hat{H}\psi_i = \epsilon_i \psi_i, \tag{3}$$

where $\hat{H}$ is the Hamiltonian of the system and ϵ_i and ψ_i are an eigenvalue and eigenvector of the Hamiltonian. The charge density and total energy of the system can be obtained from the eigenvalues and eigenvectors, along with the forces on the individual atoms. The solution of this equation depends on the formalism (tight binding, density functional theory) and basis set (atomic-like orbitals, plane waves, etc) and has been described in great detail elsewhere [175, 176].

A recent development in this field that is relevant to nanowires, and nanoscale modelling in general, is that of linear scaling (or $\mathcal{O}(N)$) methods. The computational effort required by normal implementations and techniques scales with the cube of the system size (and the memory required scales with its square). This is either due to the need to diagonalize a matrix (to find the eigenvalues and eigenvectors), which is an inherently $\mathcal{O}(N^3)$ operation, or to orthogonalize the bands (which requires an integral over all space of the product of two eigenvectors, each term of which contributes a factor of N). Thus for *ab initio* methods an effective limit of maybe 1000 atoms is placed on system sizes that can be studied, even with massively parallel computers. However, there are good reasons for believing that this cubic scaling is unnecessary. Electronic structure is essentially a local property, meaning that the memory and computational effort should only depend on a local volume around each point in the system, and hence scale linearly with the system size. It is this property that linear scaling methods use. An excellent review of the field has been written [177]; it is worth noting that most successful implementations work at the computationally more simple level of tight binding. More recent reviews of progress in developing *ab initio* techniques with linear scaling properties can be found elsewhere [178, 179].

Density functional theory and related techniques, while extremely successful, do not address various classes of problem, for instance (and most importantly) excited states or strong correlations. There are two recently emerging techniques which address excited states, among other things: GW (which takes, in general, a DFT band structure and calculates corrections arising from electron self-energy) and time-dependent DFT (which calculates the response of the electrons to a time-dependent external potential). These two techniques have been thoroughly described and compared recently [180]. For strong correlations, there are other solutions, such as the LDA + U method, which adds a Hubbard U term to the local density approximation to DFT [181] or the dynamic mean field theory (DMFT) method [182]. Possibly the most accurate many-body technique available to physicists, particularly for the solid state, is quantum Monte Carlo [183], which can also be used to provide excitation energies, though this is harder than ground-state energies.

While these methods suffice for understanding the atomic and electronic structure of nanowires, the modelling of the conduction properties (and the effects of current on the system) requires a significant change in approach. In this case, we need to model *open boundaries*, allowing the system of interest to exchange particles and energy with an environment. Since current-carrying electrons are not in the ground state, we cannot use the variational principle in the usual way [184].

3.2. Modelling conduction

The theory and calculation of conductance for nanoscale and mesoscopic systems was transformed by two key observations due to Landauer.

- The potential drop across a conductor can be viewed as arising from the self-consistent build-up of carriers, rather than the current arising from the applied electric field [185] (this paper has been reprinted in a more accessible journal [186]).
- The conductance of a device can be calculated from the electron transmission through it [27].

A brief overview of these ideas and their development is given in a review [187]. It is worth noting that these ideas are applied both at the atomic-scale level and at the mesoscopic level.

If we have a device with a number of transverse eigenstates, then the conductance (G) can be found using

$$G = \frac{2e^2}{h}\,\mathrm{Tr}(tt^{\dagger}), \tag{4}$$

where t is the transmission matrix for the device. (It should be noted that for extremely small devices there are small corrections to this formula [188].) This formula can be derived by taking the zero-frequency limit of the Kubo formula [28, 189] and by generalizing Landauer's original arguments to large system sizes [190], though, more generally, it can be derived for systems with interacting (or non-interacting) electrons using the non-equilibrium Keldysh formalism [191]. One important effect on transmission and the calculation of conductance is the narrowing of the leads [192, 193] which has a significant effect on the scattering states.

The history and development of these ideas is rather interesting. The famous Landauer formula first appeared in 1970 for a single channel [27], giving the relation $G = (e^2/\pi\hbar)T/R$, with T and R the transmission and reflection coefficients for the channel. An important point to note is that this original derivation allows for dissipation, irreversibility, etc, but places these phenomena in the leads. The formalism was later generalized to multiple channels [188] and multi-terminal samples [194]. The extension to multi-terminal samples (in 1986) also relaxed the slightly restrictive assumption by Landauer that the sample or conductor of interest was short compared to the inelastic length of electrons. A further extension to regions with interacting electrons was made in 1992 [191]. The technique is extremely well described and introduced by Datta's well-known book [195]. The Landauer formula has been recently derived using only the microscopic Kubo–Greenwood theorem, which guarantees the fluctuation–dissipation theorem and yields a finite conductance, without the need for any of the assumptions which traditionally underlie Landauer's work [28].

The accurate calculation of the transmission matrix is perhaps the key remaining problem. It can be found in terms of Green functions and terms coupling the leads to the device as [191, 196–198]

$$\mathrm{Tr}(tt^{\dagger}) = \mathrm{Tr}[\Gamma_{\mathrm{L}} G^{\mathrm{r}} \Gamma_{\mathrm{R}} G^{\mathrm{a}}], \tag{5}$$

where $\Gamma_{\mathrm{R(L)}}$ is the coupling to the right (left) lead and $G^{\mathrm{r}(a)}$ is the retarded (advanced) Green function for the device. The application of mesoscopic modelling to the calculation of the Green function is introduced thoroughly by Datta [195]; here we will consider atomistic electronic structure calculations. Two recent reviews [19, 199] summarize progress in different parts of this broad field.

There are two main routes for finding the conductance from electronic structure calculations in common use. The first works directly with Green functions, using Keldysh

non-equilibrium Green functions (NEGF) [191, 196], and building the charge density from these functions to achieve self-consistency [200–202]:

$$\hat{\rho} = -\frac{\mathrm{i}}{2\pi}\int \mathrm{d}E\, G^{<}(E), \tag{6}$$

with the lesser Green function given by

$$G^{<} = G^{\mathrm{r}}\Sigma^{<}\,[f_{\mathrm{L}},\, f_{\mathrm{R}}]\, G^{\mathrm{a}}, \tag{7}$$

where G^{r} and G^{a} are, again, the retarded and advanced Green functions of the device and $\Sigma^{<}$ represents charge injection from the electrodes and can be calculated in terms of the self-energies due to the coupling to the leads ($\Gamma_{\mathrm{L(R)}}$ in equation (5) above); $f_{\mathrm{L(R)}}$ represents a distribution function for the electrons in the left (right) lead, and will depend on channel and momentum of the wavefunction.

Practically, the charge density for the device and electrodes, $n(\mathbf{r})$, is found from the density matrix:

$$n(\mathbf{r}) = \hat{\rho}(\mathbf{r}, \mathbf{r}). \tag{8}$$

Then the potential for the system is found from this charge density, allowing a self-consistent iteration between Green functions and potential. Once a self-consistent solution is found, equations (4) and (5) can be used to generate a conductance. Alternatively, the current can be calculated directly from the transmission, thus:

$$I = \frac{2e}{\hbar}\int_{\mu_{\mathrm{L}}}^{\mu_{\mathrm{R}}} \mathrm{d}E(f_{\mathrm{L}} - f_{\mathrm{R}})T(E). \tag{9}$$

The second method in common use considers the incoming and outgoing wavefunctions from the electrodes and applies scattering theory to them, treating the 'device' of interest (be it an atomic chain or a molecule) as a perturbing potential [197–199, 203, 204]. Then the Lippmann–Schwinger equation is used, giving for one state

$$\Psi(\mathbf{r}) = \Psi_0(\mathbf{r}) + \int \mathrm{d}\mathbf{r}'\,\mathrm{d}\mathbf{r}''\, G^0(\mathbf{r}, \mathbf{r}')\delta V(\mathbf{r}', \mathbf{r}'')\Psi(\mathbf{r}''). \tag{10}$$

Here $\Psi_0(\mathbf{r})$ is the wavefunction for the leads *without* the device, and $G^0(\mathbf{r}, \mathbf{r}')$ is the Green function for the same system. $\Psi(\mathbf{r})$ is the wavefunction for the system including the device, and $\delta V(\mathbf{r}', \mathbf{r}'')$ is the *change* in potential due to the device being added. As before, we can generate a charge density (this time from the wavefunctions, $n(\mathbf{r}) = \sum_n |\Psi_n(\mathbf{r})|^2$) and hence a potential and iterate to self-consistency. The current is then found directly as

$$I = \int \mathrm{d}^2\mathbf{R}\hat{z}\cdot\mathbf{j}(\mathbf{r}) \tag{11}$$

$$\mathbf{j}(\mathbf{r}) = -2\int_{E_{\mathrm{FL}}}^{E_{\mathrm{FR}}} \mathrm{d}E\ \mathrm{Im}[\Psi(\mathbf{r})^*\nabla\Psi(\mathbf{r})]. \tag{12}$$

Here, $\mathbf{j}(\mathbf{r})$ is the current density, $\hat{z}$ represents the direction of the current flow (perpendicular to the surface of flat electrodes), and $E_{\mathrm{FR(L)}}$ is the Fermi level in the right (left) electrode.

One difference between standard electronic structure calculations and conduction calculations is the effect of the current on the electronic structure, which has been addressed by two recent theories [205, 206]. However, the major difference between these calculations and more standard electronic structure calculations, as alluded to earlier, is that of the boundary conditions: a conduction calculation requires open boundaries, which are generally represented by semi-infinite electrodes held at a particular bias. For both methods described above it is relatively easy to calculate the structure of the semi-infinite electrodes: for the first, NEGF-based method a Green function for the semi-infinite electrode is readily found from standard

techniques; for the second, Lippmann–Schwinger-based method the solution deep in the electrode is a plane wave plus the component scattered from the surface. Once these have been found, they are linked to the system of interest in the ways indicated above in equations (7) and (10). The modelling of the electrodes is approached in two ways: either using atomic detail, or via jellium of the appropriate density, capped by a layer or two of the appropriate atoms [203, 207].

The effect of electrodes and modelling them correctly is important. It has been shown that the narrowing from full, three-dimensional electrodes down to the device region can have a large effect on the overall behaviour of the conductance [192, 193, 208]. Recent models using large clusters to represent the electrodes [38, 46] found that there was no need to apply an external, sloping potential across the device as this arose from the electrostatics due to the differently charged electrodes (which have different Fermi levels). In the context of current-induced heating (discussed below in section 3.4) it has been shown [209] that good thermal contact between the device and the electrodes is important, otherwise large local heating can occur.

Various electronic structure techniques have been applied to the calculation of the Green functions, the transmission coefficients and the current in the system. They include tight binding methods [199, 210–217], some of which have been extended to include the important effects of self-consistency [212, 216–219]. There are now increasing numbers of calculations based on density functional theory (DFT) techniques [37, 42, 202, 203, 207, 220–224] exploiting different basis functions. One recent proposal [225] takes a standard periodic calculation, calculates maximally-localized Wannier functions as a basis set from the wavefunctions, and uses a standard tight binding technique [215] to calculate zero-bias conductance.

3.3. Forces and conduction

The Hellmann–Feynman theorem is commonly used in electronic structure calculations to find the forces on the ions (augmented where necessary by forces which arise due to finite basis sets). This theorem is extremely important, and has allowed the huge growth in electronic structure calculations over the last thirty to forty years. It applies to electrons in the ground state, to situations of thermal equilibrium and to the Ehrenfest regime (where ions are treated classically while electrons are treated quantum mechanically). These criteria, of course, do not apply when a non-zero bias conduction calculation is performed. There have been two considerations of how to make the Hellmann–Feynman theorem apply generally to the systems in which we are interested [226, 227], which both elegantly solve the problem of how formally to define a force in a non-equilibrium open system.

Using these formalisms it is possible to calculate some of the effects of the current on the device, notably current-induced forces which can be found from tight binding [228] (though this paper considers *ab initio* calculations initially, and only later restricts itself to tight binding) and DFT [226]. The charging and deformation of molecules (including the formation of defects such as solitons) has been considered to some extent [216, 217], and also as described in section 4.5, though the latter description was for a closed system. However, any molecular dynamics carried out on the atoms of the device under the influence of these current-induced forces is necessarily adiabatic: some form of Born–Oppenheimer approximation is followed. For each atomic configuration, the electronic structure is solved and populated appropriately, after which the forces are found and atoms moved.

3.4. Time dependence

There are a number of issues needing resolution which stand out: the problem of adiabatic evolution of ions mentioned in the last section; the need to model charged defects and their

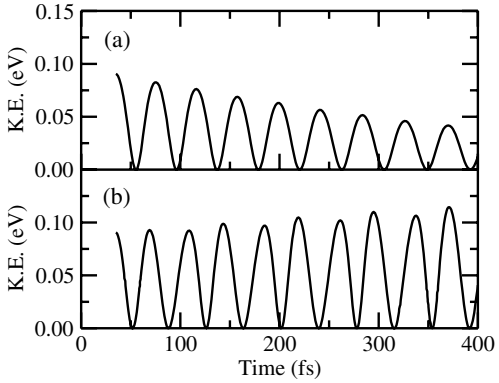

Figure 5. The variation of the ionic kinetic energy of the mobile atom with time for a bias of (a) 0.1 V and (b) 1.0 V. The initial temperature is about 600 K.

transport (there is good evidence that this will have an important role in transport for conjugated polymers [217, 229] and solid-state wires [230, 231]), which involves highly non-linear effects due to electron–phonon coupling and requires a method that can handle the electrons and ions on an equal footing; and the fact that first principles methods based on *static* DFT are challenged by the well-documented errors that it introduces for excited states, which calls into question the validity of current calculations using this technique.

A general theory for time-dependence and mesoscopic systems has been developed [232] which extends the earlier NEGF formalism [191]. An atomistic, electronic structure technique based on time-dependent density functional theory would have the advantage of standing on solid foundations for excited states, and enabling consideration of non-adiabatic effects. Formalisms for this have been suggested [233] and derived specifically for tight binding [227] and DFT [234, 235]. There have been a few practical applications of these ideas: a simulation of correlation in a resonant-tunnelling diode [236]; a study of an ethylene molecule connected to two gold electrodes by sulfur atoms [234]; and a study of C_3 between jellium electrodes [235].

There have been attempts to model current-induced heating within the adiabatic approach [209, 237, 238]. These approaches use perturbation theory to calculate heating and power dissipation, modelling the ions in two different ways: as oscillators [237, 238] and as coupled to the full phonon spectrum [209, 239, 240]. Comparing the approaches [240] found that the two schemes produced very similar power estimates except at low voltage and lattice temperatures, where the full phonon spectrum is important. These perturbative approaches are very successful (particularly in the realm of inelastic current–voltage spectroscopy, described in section 4.5). However, for larger voltages, higher order perturbation theory or non-perturbative schemes may be needed, and any attempt to investigate non-adiabatic effects requires some form of time-dependence.

One non-perturbative, time-dependent scheme has been developed very recently: a formalism for open-boundary Ehrenfest molecular dynamics [233]. This allows the electrons and ions to evolve simultaneously (though the ions are purely classical), leading to current-induced heating. Figure 5 shows the kinetic energy of a single mobile ion for two different bias voltages: 0.1 and 1.0 V. The system is modelled with a simple tight binding model; the mobile ion has a raised on-site energy to act as a barrier to current flow, while the ions in the leads are fixed and cannot transport heat away. For a small bias (0.1 V) the ionic kinetic energy decays with time (cooling), while for a large bias (1.0 V) the kinetic energy increases

(heating). The energy ($\hbar\omega$) associated with the vibrational frequency of the ion is 0.055 eV, and equals the Born–Oppenheimer surface separation for allowed transitions. Hence the change in bias increases approximately tenfold the number of possible heating transitions, producing the observed change in behaviour. Related to this is a measurement of the onset of electron–phonon interaction in monatomic gold wires [241], described in detail in section 4.5. This experiment is relevant to the both to the non-perturbative scheme and the perturbative one, where it has been modelled with excellent quantitative agreement [239].

However, this non-perturbative, time-dependent scheme is also insufficient, as the Ehrenfest approximation removes any correlation between ions and electrons arising from quantum effects. These effects are extremely important, and are responsible for part of the heating process. However, re-instating them within the Ehrenfest approximation is extremely hard, and using a level of approximation beyond Ehrenfest introduces many-body effects which are extremely hard to model (though some related work will be described in the next section). Clearly, further work is needed in this field.

3.5. Effects of electron–phonon coupling

The heating calculations described above are the simplest ways of modelling electron–phonon coupling. The ions are treated classically, and the electron–phonon interaction is taken from the model used for the electronic structure. We will see more examples of how these types of simple calculations can give interesting results for solid-state systems in section 4.5.

Of course, ions are really quantum objects, and a proper treatment of phonons requires them to be quantized. However, this makes the problem enormously more complicated, and requires simpler physical models. It is not the remit of this work to detail the field; however, there are one or two notable results. The effect of quantum polarons on electrons undergoing inelastic quantum transport has been studied [229, 242–244], and found to be potentially large; more detail will be presented in section 4.5. Recently, the Holstein polaron has been studied by a number of different methods [245–248], all of which have different regimes where they are applicable.

3.6. Effects of electron–electron coupling

It has been noted [205] that molecular conduction and structure depend strongly on the charge distribution, and that in these systems electron–electron correlation may be important and have a large effect on the conductance. It is therefore important to consider briefly work in this area, though there is little of direct relevance. The TDDFT modelling mentioned above (of a simple RTD device [236] and a molecule [234]) contained some correlation effects. We also note that the NEGF formalism [191] was derived considering electron–electron correlations as well as other effects. In section 4.5 we will briefly discuss simulations of a Luttinger liquid on a surface [249].

4. Key results

4.1. Quantized conduction and point contacts

The key characteristic of experiments measuring the conductance of a nanowire while it is being elongated is that there are sudden jumps in conductance, which correlate with discontinuities in the force. In the limit of a single quantum of conductance, chains of single atoms are formed [250]; the structure of the final plateau before fracture has been studied in detail for

Au, Al and Pb [44]. Recent measurements on copper wires [251] find that, even in a non-magnetic material, it might be possible to lift the spin degeneracy and halve the fundamental quantum of conductance (an effect observed in magnetic constrictions).

It is now widely accepted that the jumps in conductance are due to rearrangements of the atomic structure of the wire. There are various pieces of evidence: real-time TEM measurements of the formation and breaking of a gold nanowire [252]; TEM measurements and conductance measurements during the elongation of a gold nanowire [35]; TEM measurements of the electronic structure and conductance of gold nanowires and semi-empirical calculations of the resulting deduced atomic structures [253]; and DFT calculations of the rearrangement and conductance of a stretched nanowire of Na [254] and Al [255]. All of these studies confirm this interpretation. For more details on this, and other aspects of quantum point contacts, the interested reader is referred to the recent review of the field [1].

The atomic structure of the gold chains viewed in a TEM has caused some controversy; the spacing deduced is around 3.0–3.5 Å [35], while modelling results suggest that the spacing should be ∼2.7 Å [256, 257]. Other experimental measurements, however, found results more in line with theoretical modelling (2.3–2.7 Å [36] and 2.5–2.9 Å [258]). Various suggestions have been made to explain the discrepancy: an unexpectedly large workfunction due to He affecting calibration of the TEM [36]; spinning zig-zag chains of Au [257] (though recent TEM measurements suggest that this is not possible [259]); and the presence of impurities such as H or S [260], C [261] or O [262]. A definitive answer to this problem has yet to be found. A related DFT study of the structure of infinite chains of various metals (Au, Al, Ag, Pd, Rh, Ru) [263] offers useful insight to some of the issues.

Given sufficient stretching, or a large enough current passing through it, a wire will break. This has been observed in experiment [33, 34, 250, 264], and modelled using both normal, mechanical considerations [256, 265, 266] and current-induced forces [267]. Most interestingly, it is found that the current-induced forces are not large enough themselves to break the chain, but embrittle it so that thermally-activated spontaneous fracture is much more likely.

By contrast to these free chains, the electronic structure of one-dimensional, monatomic chains on metal surfaces has been studied using STM (both to assemble and characterize the chains) for Au on NiAl(110) [268–270] and Cu on Cu(111) [271]. These chains, whose transport and mechanical properties are not considered, are modelled remarkably well by a simple, 1D particle-in-a-box model.

4.2. Single molecule conduction

One of the first measurements of the conductance of a molecule was for benzene-1,4-dithiol between gold electrodes [113]. The modelling results for this molecule are varied: early results found that while the overall shape of the differential conductance was well reproduced, the magnitude was much too large [204, 272]. A more recent study [273] suggests that the current path measured in experiment may have involved *two* molecules; their simulations for this path match the measured results well. A study of the effects of current-induced forces [274] found that up to about 5 V there is little effect on the current flowing, though the molecule starts to change conformation. There have been many other studies of related molecules, for instance xylyl [210, 272] and various thiophenes [275–278]. These calculations all find that both the bonding site (on-top or hollow) and the bonding nature (through an S atom or an H atom) to the electrodes can affect the conductance greatly. Other calculations concentrated on the effect of the angle between the molecule and the substrate [279, 280], which is found to change the conductance by up to an order of magnitude. The transport through a large molecule lying *flat*

on the Au(001) surface via STS shows that it is possible to identify some of the orbitals of the molecule [281].

The nature of the gold–sulfur bond has been studied by simulating the removal of an alkane thiolate from a gold surface [282]; rather than rupturing the molecule–gold bond, it was found that gold atoms were pulled out of the surface, forming a gold nanowire which eventually ruptures. This suggests that experimental measurements of conductance 'switching' which has been attributed to conformational changes of the molecules [114, 115] and to the mobility of the molecules across the gold surface [116] is unlikely to be due to the latter mechanism. The large, unanswered question that remains here relates to the contact between the molecule and the junction: it is not clear what the experiment is measuring, which makes simulations very hard to perform. One route to further understanding this problem lies in detailed, atomic-scale imaging of metal–molecule junctions [283].

As well as studying the conductance of single molecules, nanoelectronic devices have been created, using a single molecule as the active part [284]. While nanoscale logic is covered in the next section, it makes sense to detail the progress with logic elements made from single molecules here. At the simplest level, rectification has been observed using molecules [111, 285], but more interesting results have been achieved. A molecule consisting of three linked benzene rings with nitro and amine groups on the central ring was found to have a large negative differential resistance, which was washed out with increasing temperature [286]. This was modelled successfully [276], with the change of behaviour with temperature being attributed to the excitation of rotational modes in the molecule. A similar molecule has been used in a random access memory cell [287]: the device is 'written' with a voltage pulse of up to 5 V, and shows a bit retention time of 15 min at room temperature. A different class of molecules (rotaxanes) has been used to create logic gates (AND and OR, though only single use gates) [10] and a reconfigurable switch [11]. A robust molecular memory based on porphyrin molecules on Si(001) has been demonstrated [288]; these are unaffected by repeated usage and environmental extremes (surviving baking at 400 °C and up to 1000 read/write cycles), pointing the way towards integration with conventional electronics.

4.3. Nanoscale logic

An obvious application of nanoscale wires and objects is to electronic components (or logic components) on the nanoscale. We have already described the use of single molecules in nanoscale logic in the previous section. Using carbon nanotubes [289, 290] or semiconductor nanowires, field-effect transistors and logic circuits of various descriptions have been built. The components created include rectifiers (from CNTs [3, 157] and semiconductor NWs [156, 157, 162, 291]); FETs (from CNTs [4, 13, 143, 292–299] and semiconductor NWs [155, 160, 297]); inverters (using CNTs [13, 14, 294] and semiconductor NWs [291]); single-electron transistor (NWs [300]); and NOR gate (using CNTs [14] and semiconductor NWs [12]). A suggestion for random access memory using carbon nanotubes [301] uses both electronic and elastic properties of the tubes, but is highly speculative. These various demonstrations and proposals show the potential of nanoscale wires for electronic applications, but have not yet achieved a level of control or integration suitable for useful applications. However, one important step, the question of addressing individual components, has been considered [297]: by chemically modifying semiconductor NWs and assembling them in a crossed array, independent addressing and demultiplexing have been demonstrated.

As well as electronic applications, there are light-based applications. Carbon nanotubes have been shown to emit in the infra-red when holes and electrons are injected [298], while nanowires have been shown to emit light [154, 155, 174] and to lase (given a suitable cleaving so that the ends of the wire act as mirrors) [163, 170, 171].

4.4. Spin transport

A major growth area of both research and application is that of spin electronics, or spintronics, where the ability to manipulate up and down spin electrons differently is used as well as the ability to manipulate charge; the first suggestion for this area involved a spin FET [302]. There are large areas of application in metallic systems and ferromagnetic semiconductors (e.g. Mn-doped GaAs): information on these areas can be found in a number of reviews [303–309]. One effect of note is the reversal of magnetization in magnetic nanowires [310]; this is a high current effect (10^7–10^8 A cm^{-2}), but has huge potential, as purely electrical switching of magnetization has long been sought after in the field of information storage. Recent work has found that the analogous domain-wall switching in a ferromagnetic semiconductor [311] can occur at lower current densities (10^5 A cm^{-2}). Modelling relevant to this field has been well reviewed [312]; of particular interest is work that shows that, with spin-polarized transport, some electron–electron interactions which are irrelevant in normal transport can have a significant effect [313].

There is also growing interest in spin transport within the field of atomic-scale wires. There is theoretical work which suggests that the almost canonical benzene dithiolate molecule will work as a spin-valve when attached to Ni electrodes [314], as well as a prediction that DNA will show magnetoresistance ratios of 26% and 16% when attached to Ni and Fe electrodes, respectively [315]. Recent experiments on spin transfer between quantum dots found that organic molecules attached to semiconductor quantum dots transferred spin along the π-conjugated bonds [316]. Spin transport has also been measured along carbon nanotubes with ferromagnetic contacts [317–319]. These experiments found a magnetoresistance ratio of about 10% (in good agreement with theoretical modelling [320]) and spin coherence over 130 nm. Finally, we must mention spin polarized STM [321], which allows imaging of magnetic moments on the atomic scale.

4.5. One-dimensional conduction: electron–phonon and electron–electron effects

The phenomenon of electron–phonon coupling and its effects on conduction are well studied in conducting polymers (often modelled with the Su–Schrieffer–Heeger model [322]) where polaronic transport can dominate; an understanding of charge transport in conjugated polymers has been recently reviewed [323]. The quantum inelastic conductance of conjugated polymers has been calculated non-perturbatively [229], showing that at low energies, i.e. in the gap, the tunnelling current *increases* relative to the current calculated using just elastic scattering. The mechanism behind this is quantum coherent transport of polarons, which arises from the electron–phonon interactions in the system. Figure 6 shows the atomic displacements resulting from an electron tunnelling along a 100 site polyacetylene chain, plotted against electron position (left panel) and against chain position (right panel, with different electron positions indicated using different curves). Note in particular the distortion associated with the electron, and the 'wake' left behind as the electron travels along the wire, seen in the right panel.

Recently, low temperature measurements of conduction in monatomic gold wires at very low bias voltages provided direct observation of the onset of electron–phonon coupling [241, 324]: no dissipation was observed until the bias reached about 12 meV (an energy which is dependent on strain and wire structure), which is the energy of the first zone-boundary phonon. This phenomenon has been studied recently theoretically. Using DFT [209], the onset voltage was successfully reproduced, and the method also applied to a benzene dithiolate molecule. With tight binding [239], good quantitative agreement was

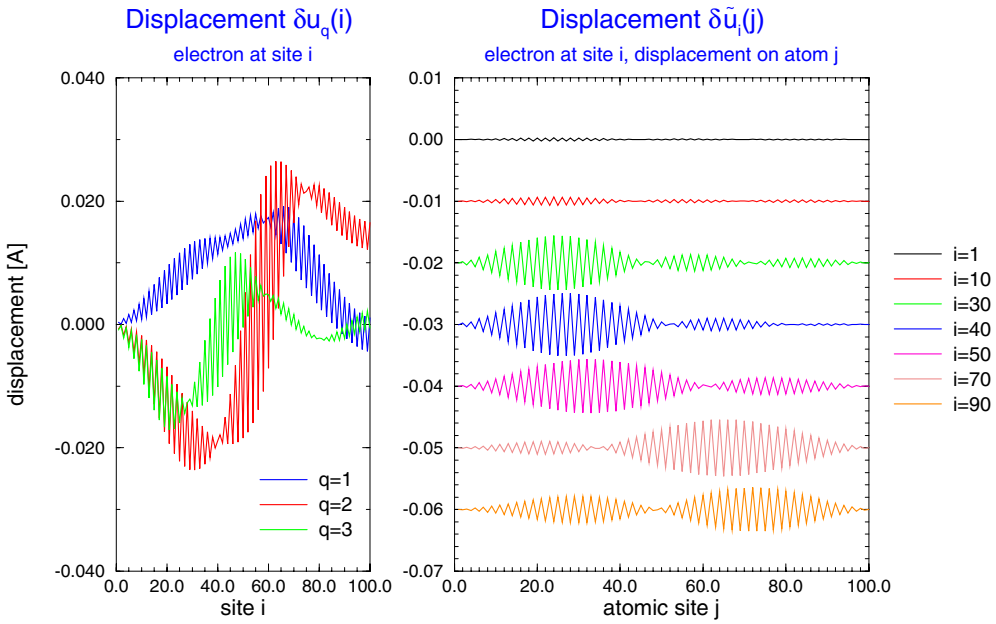

Figure 6. Displacement due to a tunnelling electron (injection energy at mid-gap) for a 100-atom polyacetylene chain, plotted from two points of view. Left panel: displacement of phonon mode (vertical axis) plotted as a function of electron displacement (horizontal axis) for the lowest three phonon modes. Right panel: displacement of atom (vertical axis) plotted as a function of distance along chain (horizontal axis) for different values of electron position, given by different curves. The different electron curves are shifted vertically by 0.01 for clarity. The electron propagates from left to right in both cases. *Image courtesy of Andrew Fisher*.

found for the onset voltage and the change of this voltage with tension in the wire. This is only one example from the field of inelastic current–voltage spectroscopy. (More details of STM studies of molecules using this technique can be found in a recent review [22].)

The dangling bond wire described in section 2.2 is an intriguing example of a solid-state system where electron–phonon coupling is important for conduction. It consists of a dimer row on Si(001) with the dimer atoms on one side of the row passivated with hydrogen; the clean dimer atoms undergo a Peierls distortion, resulting in alternating 'up' and 'down' atoms and charge transfer from 'down' atom to 'up' atom. At first sight, the system should have some similarities to the conjugated polymers, with the alternation of 'up' and 'down' analogous to the single–double bond alternation; in actual fact, the differences are rather interesting.

Injecting charge results, as expected, in formation of a polaron [230]. The location of the polaron depends on the charge carrier: an electron will localize on a charge-poor 'down' atom, while a hole localizes on a charge-rich 'up' atom. In both cases, the Peierls distortion is locally reduced. Analysis of the phonon modes of the system shows that the polaron is weakly coupled to the substrate [230], leading to the expectation that it ought to be reasonably mobile. Modelling of diffusive, temperature-induced motion of hole polarons in DB wires [231] found that the polarons had a mobility of 7.19×10^{-5} m^2 V^{-1} s^{-1}, which is an appreciable mobility despite the self-trapping of the hole. The position of the hole along the wire for two temperatures is shown in figure 7. We see that at a low temperature (200 K) the polaron hops a few times, and is generally localized on a single 'up' atom, though this is distorted towards the 'down' position. (The 'up' atom positions are indicated with dashed

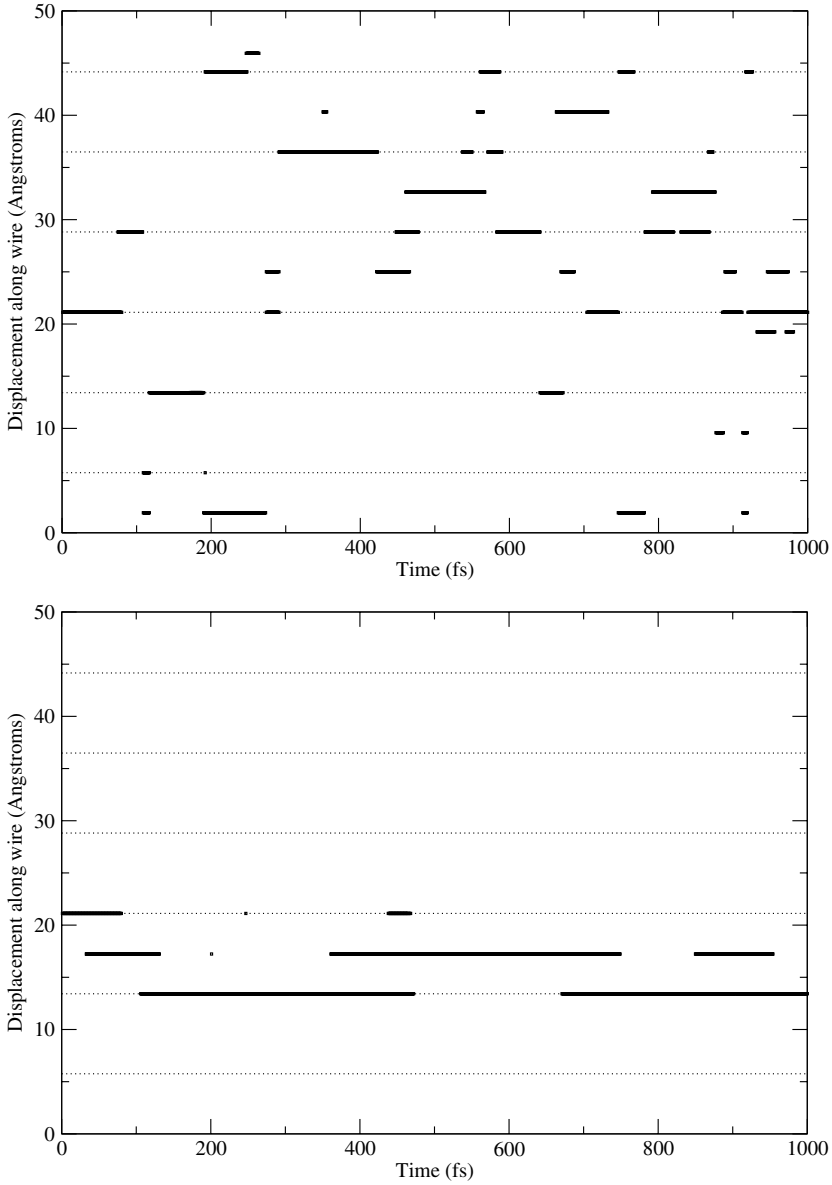

Figure 7. Displacement of a hole polaron along the DB wire as a function of time for $T = 200$ K (lower panel) and $T = 700$ K (upper panel). Dashed lines across the page indicate the location of the 'up' atoms in the DB wire (where the polaron localizes at 0 K) and are separated by two dimer spacings, or 7.68 Å.

lines.) At a high temperature (700 K), by contrast, the polaron is much more mobile, spreading out over several atoms at various points. However, the polaron remains fully localized on one atom (with the majority of its weight on that atom) until a temperature where the hydrogen on the Si(001) surface would be desorbing. The diffusion of these polarons ought to be observable at room temperature. Effects associated with conjugated polymers such as solitons are also observed [325], though they take a different form. Instead of alternation of 'up'

and 'down' atoms along the chain, there are pairs of adjacent 'up' or 'down' atoms. These have gap states associated with them, as expected, but they differ from the mid-gap states seen in polymer solitons: for the 'up–up' soliton, the state is localized near the top of the valence band, while the state for the 'down–down' soliton is localized near the bottom of the conduction band. These examples demonstrate the importance of electron–phonon effects even in solid-state systems, and the change in electronic structure and conduction properties that they can induce.

Another important area is that of electron–electron correlations, which results in phenomena such as Luttinger liquid behaviour and the Kondo effect. As already discussed in section 2.5, there is now both direct and indirect evidence of Luttinger liquid behaviour in carbon nanotubes. In a related field (that of two-dimensional electron gasses), chiral Luttinger liquid behaviour has been measured [326, 327]; this field is thoroughly reviewed elsewhere [328]. While the theory of the Luttinger liquid is well understood (there is an excellent review of the subject [329]), the effects of a surface on a one-dimensional system are poorly understood. One examination of this area used two coupled chains of atoms (one with correlations to represent the Luttinger liquid, and the other without, to represent the surface) [249]. The results are intriguing, showing that there are both Luttinger and Fermi liquid characters present in the coupled system. Specifically, while the Luttinger liquid parameters show departure from Fermi liquid values, the charge distribution between the two chains (particularly with strong coupling between the chains) starts to show a Fermi liquid-like neutral excitation spectrum. Another example of behaviour due to strong electron–electron correlations, the Kondo effect, has been measured in individual molecules [120, 121], making it clear how easy (relatively) it is experimentally to achieve levels of high correlation which may be challenging to model. Theoretical approaches to modelling the Kondo effect in Coulomb-blockaded quantum dots (including CNTs and molecular transistors) have been recently reviewed [330].

4.6. Growth and assembly

The problem of accurate growth and assembly at the atomic scale is a formidable one: even if methods for controlling structures at this level are developed, it is unlikely that they would survive processing, encapsulation and operation at elevated temperatures without change. The question of whether this level of control is desirable or even necessary will be considered in section 5, while in this section we will examine techniques and results for alignment.

For the semiconductor nanowires of section 2.6, two methods have been investigated for depositing and aligning them. Alignment using electrical fields is possible [162, 331] though use of microfluidics gives better control and is easier [332]. In the electrical field alignment technique [331], a drop of nanowire solution is deposited on electrodes which are then biased (often with high voltages, up to 100 V). By varying the electrodes, and using layer-by-layer deposition techniques, a variety of geometries are possible. The microfluidic technique, by contrast, uses channels in polymer moulds to pass suspensions of NWs over a substrate. This results in ordered arrays of NWs (with better angular control gained with higher flow rates) which can be arranged in different patterns (e.g. crossed) by sequential deposition steps at different angles. Both techniques can be combined with surface pre-patterning to improve or change deposition locations. Applications of these techniques have been discussed in section 4.3.

Another promising technique for assembling wires arises from the discovery that epitaxial islands of $TiSi_2$ on Si(001) and Si(111) will act as catalysts, leading to silicon nanowires growing on a silicon substrate [158]. A similar technique has been recently developed for

CNTs: they grow off nanoscale catalyst particles, directly on the substrate [144]. Alternatively, a recent demonstration of functionalization of CNTs [147] has opened the way to controlling the deposition of nanotubes through site-specific reactivity and binding.

While self-assembly is often associated with biological systems, we have touched on various inorganic self-assembled systems, which would be useful either if ways of controlling the assembly could be found, or in the context of using randomly placed wires (discussed in section 5). The rare-earth nanowires and Bi nanolines discussed in section 2.3 are the two most obvious candidates for these systems. The Bi nanolines, which are not conducting, have been shown to be resistant to attack by radical H or O [88], which suggests that they might be useful as templates (for instance, masking the reactive Si(001) surface with hydrogen and adsorbing metal as done for DB wires, or oxidizing the substrate). We have also mentioned nanolithography, which is too intensive to be of any practical use. However, further application of the self-propagating styrene wires might be one possible route to using scanning probes. A proposal for high density nanowires with small diameters and pitches uses a GaAs/AlGaAs superlattice [333]. The AlGaAs is etched away, and metal is evaporated obliquely, giving wires which are transferred to a prepared substrate by adhesion.

Returning to biological assembly, increasing use is being made of the self-assembling properties of DNA, and its sequence specific binding. Many of these applications are larger scale than the systems that have been considered in this review, but two deserve mention. The first uses crosses of DNA to assemble a square lattice on a substrate which can be subsequently metallized [334], though this is not the first time that DNA has been used as a template for metal deposition. The second uses DNA to bind to CNTs [299] which then self-assemble, for instance into a field-effect transistor capable of operation at room temperature.

As well as assembling or growing nanowires of different descriptions, it is important to consider the effect of encapsulation for later use. We have already mentioned the cyclodextrin sheath [124] which can be used essentially as insulation for a semiconducting polymer. The efficacy of this system has been demonstrated in the real-world application of organic LEDs [126]. Of course, other systems exist: the growth of Ag nanowires in an organic complex [335] has been shown to result in electron density localized on the silver [336]; with CNTs, there are 'peapod' nanotubes [337], where C_{60} (and related fullerenes) are encapsulated in a nanotube, and BN sheaths for C_{60} and CNTs [338]. Work on doping CNTs by encapsulation of organic molecules [339] can also be used to protect the molecules within the CNT sheath (as modelled for polyacetylene [340]). There is also work on nanocrystals of various inorganic compounds encapsulated in SWNTs [341].

5. Conclusions

There is a very real commercial drive behind the development of nanometre-scale wires and electronic components. In this review, I have surveyed various interesting and promising systems which, as well as being candidates for this commercial application, hold their own interesting scientific questions and properties. A key property of many of the systems is that as well as being candidates for nanoscale wires, they also have the potential to form the active part of a device, yielding gain (indeed, a recent Japanese government project, which has looked at some of the systems in this review, had the title 'Active Atom-Wire Interconnects'). This ability to be both interconnect and device may well prove extremely important.

However, there are various problems and questions that remain. To my mind, the major one concerns that of control against randomness. Accurate deposition or lithography at the atomic scale is either impossible or extremely labour intensive: self-assembled systems tend to exhibit

atomic-scale fluctuations (with the exception of the Bi nanolines discussed in section 2.3). This is a problem being confronted in one solid-state quantum computing proposal [342]: the need to locate and address accurately single phosphorus atoms is extremely demanding.

However, there is an alternative approach. There have been at least two suggestions, from very different backgrounds, for working with, or even using, the randomness resulting from non-controlled deposition. First, the Teramac computer [343], which was built from a large number of extremely cheap, defective components, cross-wired in a way which was simple to implement but inherently defective. The effort in configuring the components into a useful architecture (and working around the defects) is devolved to software; the machine in one configuration achieved 10^{12} operations per second, running at a clock speed of 1 MHz. We can see how this could be applied to arrays of wires and devices deposited on a surface, though the time required for the look-up tables (LUTs) may require careful thought and algorithmic development. Second, a proposal for solid-state quantum computing [344] which uses electron spins on spatially disordered deep donors in silicon as the qubits. The qubits are coupled by optically-induced electronic excitation: two deep donors are coupled by the excited state of a nearby control impurity. For this scheme, the randomness associated with (say) ion implantation to create the deep donors and control impurities is an advantage. It means that the frequencies required to excite and couple specific sites and control atoms will differ significantly, removing the need for high precision addressing.

Without techniques such as the specialized one just described, we are still left with the need to address and contact individual nanoscale objects. The use of nanowires as both interconnect and device, coupled with various ingenious suggestions for addressing (for instance the chemical modification of nanowires [297]), may offer a way forward, but we note that in modern VLSI chips there are often seven or nine layers of interconnect, which drives the complexity of design and fabrication. Any highly integrated scheme for nanoelectronics will have this same barrier to large-scale fabrication.

Once these hurdles are crossed, the questions of robustness and ability to carry current need to be addressed. Encapsulation of a device will inevitably affect its operation, and the associated materials processing often involves high temperatures and potentially hostile environments. The long-term stability of atomic-scale wires needs careful thought: we have already seen how current-induced forces can affect these systems. The question of whether to carry a current (as modern silicon-based transistors do) or a signal (as, for instance, optical fibre does) is another key issue to be solved. It may well be that the best solution is one of complementarity and integration: using atomic-scale devices in new ways with existing technology.

Away from the technology-oriented application of the field, the most interesting challenge, which is simultaneously the biggest problem, is that of bringing experimental measurements and theoretical predictions into line. Often this is a matter of specifying the conditions: we have seen, for instance, that a small change in the contact between a molecule and the electrodes used for measuring can alter the current by an order of magnitude or more. The problem can be examined from both points of view: better routes of preparation and characterization of the electrodes and reproducibility from experiment, and expansion of theory to allow impurities, different angles and other imperfections to be modelled. Close interaction of theory and experiment is key to progress on this, and many other, fronts.

Having pointed out various problems and issues to be considered, I must emphasize that the field is enormously exciting. There is a convergence of experiment and modelling which has not been seen before: experiment is now able to address systems under conditions and of sizes where theory can make realistic predictions. There are still many unanswered questions, but this is part of what is driving the development of new techniques and ideas.

Acknowledgments

DRB thanks Andrew Fisher, Mike Gillan, Taro Hitosugi, Andrew Horsfield, Jun Nara, Takahisa Ohno, James Owen, Marshall Stoneham, Tchavdar Todorov and David Williams for useful conversations. He gratefully acknowledges permission to use images from Andrew Fisher, Taro Hitosugi, Tatsuya Narushima, James Owen and Lars Samuelson. He is supported by the Royal Society through a University Research Fellowship.

References

[1] Agraït N, Yeyati A L and van Ruitenbeek J M 2003 *Phys. Rep.* **377** 81
[2] Yeom H W *et al* 1999 *Phys. Rev. Lett.* **82** 4898
[3] Yao Z, Postma H W C, Balents L and Dekker C 1999 *Nature* **402** 273
[4] Nygård J, Cobden D, Bockrath M, McEuen P and Lindelof P 1999 *Appl. Phys.* A **69** 297
[5] Bockrath M, Cobden D H, Lu J, Rinzler A G, Smalley R E, Balents L and McEuen P L 1999 *Nature* **397** 598
[6] Durkan C, Schneider M A and Welland M E 1999 *J. Appl. Phys.* **86** 1280
[7] Durkan C and Welland M E 2000 *Phys. Rev.* B **61** 14215
[8] Yasin S, Hasko D G and Ahmed H 2001 *Appl. Phys. Lett.* **78** 2760
[9] Durkan C and Welland M E 2000 *Ultramicroscopy* **82** 125
[10] Collier C P, Wong E W, Belohradsky M, Raymo F M, Stoddart J F, Kuekes P J, Williams R S and Heath J R 1999 *Science* **285** 391
[11] Collier C P, Mattersteig G, Wong E W, Luo Y, Beverly K, Sampaio J, Raymo F M, Stoddart J F and Heath J R 2000 *Science* **289** 1172
[12] Huang Y, Duan X, Cui Y, Lauhon L J, Kim K H and Lieber C M 2001 *Science* **294** 1313
[13] Derycke V, Martel R, Appenzeller J and Avouris P 2001 *Nano Lett.* **1** 453
[14] Bachtold A, Hadley P, Nakanishi T and Dekker C 2001 *Science* **294** 1317
[15] Chen Y, Ohlberg D A A, Li X, Stewart D R, Williams R S, Jeppesen J O, Nielsen K A, Stoddart J F, Olynick D L and Anderson E 2003 *Appl. Phys. Lett.* **82** 1610
[16] Ciraci S, Buldum A and Batra I P 2001 *J. Phys.: Condens. Matter* **13** R537
[17] Ouyang M, Huang J L and Lieber C M 2002 *Acc. Chem. Res.* **35** 1018
[18] Moriarty P 2001 *Rep. Prog. Phys.* **64** 297
[19] Nitzan A 2001 *Annu. Rev. Phys. Chem.* **52** 681
[20] Nitzan A and Ratner M A 2003 *Science* **300** 1384
[21] Gimzewski J K and Joachim C 1999 *Science* **283** 1683
[22] Ho W 2002 *J. Chem. Phys.* **117** 11033
[23] Hofer W A, Foster A S and Shluger A L 2003 *Rev. Mod. Phys.* **75** 1287
[24] Kaiser A B 2001 *Rep. Prog. Phys.* **64** 1
[25] Himpsel F J, Ortega J E, Mankey G J and Willis R F 1998 *Adv. Phys.* **47** 511
[26] Ho P S and Kwok T 1989 *Rep. Prog. Phys.* **52** 301
[27] Landauer R 1970 *Phil. Mag.* **21** 863
[28] Das M P and Green F 2003 *J. Phys.: Condens. Matter* **15** L687
[29] Pascual J I, Méndez J, Gómez-Herrero J, Baró A M and García N 1993 *Phys. Rev. Lett.* **71** 1852
[30] Brandbyge M, Schiøtz J, Sørensen M R, Stoltze P, Jacobsen K W, Nørskov J K, Olesen L, Laegsgaard E, Stensgaard I and Besenbacher F 1995 *Phys. Rev.* B **52** 8499
[31] Costa-Krämer J L, García N, García-Mochales P and Serena P A 1995 *Surf. Sci.* **342** L1144
[32] van den Brom H E and van Ruitenbeek J M 1999 *Phys. Rev. Lett.* **82** 1526
[33] Yasuda H and Sakai A 1997 *Phys. Rev.* B **56** 1069
[34] Itakura K, Yuki K, Kurokawa S, Yasuda H and Sakai A 1999 *Phys. Rev.* B **60** 11163
[35] Ohnishi H, Kondo Y and Takayanagi K 1998 *Nature* **395** 780
[36] Untiedt C, Yanson A I, Grande R, Rubio-Bollinger G, Agraït N, Vieira S and van Ruitenbeek J 2002 *Phys. Rev.* B **66** 085418
[37] Brandbyge M, Mozos J L, Ordejón P, Taylor J and Stokbro K 2002 *Phys. Rev.* B **65** 165401
[38] Louis E, Vergés J A, Palacios J J, Pérez-Jiménez A J and SanFabián E 2003 *Phys. Rev.* B **67** 155321
[39] Tsukada M, Kobayashi N and Brandbyge M 1998 *Prog. Surf. Sci.* **59** 245
[40] Kobayashi N, Brandbyge M and Tsukada M 1999 *Surf. Sci.* **433–435** 854
[41] Kobayashi N, Brandbyge M and Tsukada M 2000 *Phys. Rev.* B **62** 8430

[42] Kobayashi N, Aono M and Tsukada M 2001 *Phys. Rev.* B **64** 121402(R)
[43] Kobayashi N, Brandbyge M and Tsukada M 1999 *Japan. J. Appl. Phys.* 1 **38** 336
[44] Cuevas J C, Yeyati A L, Martín-Rodero A, Bollinger G R, Untiedt C and Agraït N 1998 *Phys. Rev. Lett.* **81** 2990
[45] Cuevas J C, Yeyati A L and Martín-Rodero A 1998 *Phys. Rev. Lett.* **80** 1066
[46] Palacios J J, Pérez-Jiménez A J, Louis E, SanFabián E and Vergés J A 2002 *Phys. Rev.* B **66** 035322
[47] Sim H S, Lee H W and Chang K J 2001 *Phys. Rev. Lett.* **87** 096803
[48] Tsukamoto S and Hirose K 2002 *Phys. Rev.* B **66** 161402
[49] Brandbyge M, Sørensen M R and Jacobsen K W 1997 *Phys. Rev.* B **56** 14956
[50] Sørensen M R, Brandbyge M and Jacobsen K W 1998 *Phys. Rev.* B **57** 3283
[51] Brandbyge M, Kobayashi N and Tsukada M 1999 *Phys. Rev.* B **60** 17064
[52] Lyding J W, Shen T C, Hubacek J S, Tucker J R and Abeln G C 1994 *Appl. Phys. Lett.* **64** 2010
[53] Lyding J W, Abeln G C, Shen T C, Wang C and Tucker J R 1994 *J. Vac. Sci. Technol.* B **12** 3735
[54] Shen T C, Wang C, Abeln G C, Tucker J R, Lyding J W, Avouris P and Walkup R E 1995 *Science* **268** 1590
[55] Hitosugi T, Hashizume T, Heike S, Watanabe S, Wada Y, Hasegawa T and Kitazawa K 1997 *Japan. J. Appl. Phys.* 2 **36** L361
[56] Foley E T, Kam A F, Lyding J W and Avouris P 1998 *Phys. Rev. Lett.* **80** 1336
[57] Hitosugi T, Heike S, Onogi T, Hashizume T, Watanabe S, Li Z Q, Ohno K, Kawazoe Y, Hasegawa T and Kitazawa K 1999 *Phys. Rev. Lett.* **82** 4034
[58] Bird C F and Bowler D R 2003 *Surf. Sci.* **531** L351
[59] Adams D P, Mayer T M and Swartzentruber B S 1996 *Appl. Phys. Lett.* **68** 2210
[60] Hashizume T, Heike S, Lutwyche M I, Watanabe S, Nakajima K, Nishi T and Wada Y 1996 *Japan. J. Appl. Phys.* 2 **35** L1085
[61] Hashizume T, Heike S, Lutwyche M I, Watanabe S and Wada Y 1997 *Surf. Sci.* **386** 161
[62] Shen T C, Wang C and Tucker J R 1997 *Phys. Rev. Lett.* **78** 1271
[63] Palasantzas G, Ilge B, Nijs J D and Geerligs L J 1999 *J. Appl. Phys.* **85** 1907
[64] Butcher M J, Jones F H and Beton P H 2000 *J. Vac. Sci. Technol.* B **18** 13
[65] Sakurai M, Thirstrup C and Aono M 2000 *Phys. Rev.* B **62** 16167
[66] Hersam M C, Guisinger N P and Lyding J W 2000 *Nanotechnology* **11** 70
[67] Abeln G C, Hersam M C, Thompson D S, Hwang S T, Choi H, Moore J S and Lyding J W 1998 *J. Vac. Sci. Technol.* B **16** 3874
[68] Abeln G C, Lee S Y, Lyding J W, Thompson D S and Moore J S 1997 *Appl. Phys. Lett.* **70** 2747
[69] Watanabe S, Ono Y A, Hashizume T and Wada Y 1996 *Phys. Rev.* B **54** R17308
[70] Watanabe S, Ono Y A, Hashizume T and Wada Y 1997 *Surf. Sci.* **386** 340
[71] Yajima A, Tsukada M, Watanabe S, Ichimura M, Suwa Y, Onogi T and Hashizume T 1999 *Phys. Rev.* B **60** 1456
[72] Haye M J, Scholte P M L O, Bakker A F, de Leeuw S W, Tuinstra F and Brocks G 1997 *Phys. Rev.* B **56** R1708
[73] Lopinski G P, Wayner D D M and Wolkow R A 2000 *Nature* **406** 48
[74] Preinesberger C, Vandré S, Kalka T and Dähne-Prietsch M 1998 *J. Phys. D: Appl. Phys.* **31** L43
[75] Nogami J, Liu B Z, Katkov M V, Ohbuchi C and Birge N O 2001 *Phys. Rev.* B **63** 233305
[76] Chen Y, Ohlberg D A A and Williams R S 2002 *J. Appl. Phys.* **91** 3213
[77] Preinesberger C, Becker S K, Vandré S, Kalka T and Dähne M 2002 *J. Appl. Phys.* **91** 1695
[78] Liu B Z and Nogami J 2003 *J. Appl. Phys.* **93** 593
[79] Chen Y, Ohlberg D A A, Medeiros-Ribeiro G, Chang Y A and Williams R S 2000 *Appl. Phys. Lett.* **76** 4004
[80] Ohbuchi C and Nogami J 2002 *Phys. Rev.* B **66** 165323
[81] Lee D and Kim S 2003 *Appl. Phys. Lett.* **82** 2619
[82] Stevens M, He Z, Smith D J and Bennett P A 2003 *J. Appl. Phys.* **93** 5670
[83] Decker C A, Solanki R, Freeouf J L, Carruthers J R and Evans D R 2004 *Appl. Phys. Lett.* **84** 1389
[84] Brongersma S H, Castell M R, Perovic D and Zinke-Allmang M 1998 *Phys. Rev. Lett.* **80** 3795
[85] Owen J H G, Miki K, Koh H, Yeom H W and Bowler D R 2002 *Phys. Rev. Lett.* **88** 226104
[86] Miki K, Bowler D R, Owen J H G and Sakamoto K 1999 *Phys. Rev.* B **59** 14868
[87] Owen J H G, Miki K and Bowler D R 2003 *Surf. Sci.* **527** L177
[88] Owen J H G, Bowler D R and Miki K 2002 *Surf. Sci.* **499** L124
[89] Evans M M R and Nogami J 1999 *Phys. Rev.* B **59** 7644
[90] Dong Z C, Fujita D and Nejoh H 2001 *Phys. Rev.* B **63** 115402
[91] Li J L, Liang X J, Jia J F, Liu X, Wang J Z, Wang E G and Xue Q K 2001 *Appl. Phys. Lett.* **79** 2826
[92] Wang J Z, Jia J F, Liu X, Chen W D and Xue Q K 2002 *Phys. Rev.* B **65** 235303
[93] Kida A, Kajiyama H, Heike S, Hashizume T and Koike K 1999 *Appl. Phys. Lett.* **75** 540

[94] Zhang Y P, Yang L, Lai Y H, Xu G Q and Wang X S 2004 *Appl. Phys. Lett.* **84** 401
[95] Sunamura H, Usami N, Shiraki Y and Fukatsu S 1996 *Appl. Phys. Lett.* **68** 1847
[96] Omi H and Ogino T 1997 *Appl. Phys. Lett.* **71** 2163
[97] Kawamura M, Paul N, Cherepanov V and Voigtländer B 2003 *Phys. Rev. Lett.* **91** 096102
[98] McChesney J L, Kirakosian A, Bennewitz R, Crain J N, Lin J L and Himpsel F J 2002 *Nanotechnology* **13** 545
[99] Lin J L, Petrovykh D Y, Viernow J, Men F K, Seo D J and Himpsel F J 1998 *J. Appl. Phys.* **84** 255
[100] Losio R, Altmann K N and Himpsel F J 2000 *Phys. Rev. Lett.* **85** 808
[101] Baski A A, Saoud K M and Jones K M 2001 *Appl. Surf. Sci.* **182** 216
[102] Lee S S, Kim N D, Hwang C G, Song H J and Chung J W 2002 *Phys. Rev.* B **66** 115317
[103] Ahn J R, Yeom H, Yoon H S and Lyo I W 2003 *Phys. Rev. Lett.* **91** 196403
[104] Crain J N, Kirakosian A, Altmann K N, Bromberger C, Erwin S C, McChesney J L, Lin J L and Himpsel F J 2003 *Phys. Rev. Lett.* **90** 176805
[105] Segovia P, Purdie D, Hengsberger M and Baer Y 1999 *Nature* **402** 504
[106] Losio R, Altmann K N, Kirakosian A, Lin J L, Petrovykh D and Himpsel F J 2001 *Phys. Rev. Lett.* **86** 4632
[107] Ahn J R, Kim N D, Lee S S, Lee K D, Yu B D, Jeon D, Kong K and Chung J W 2002 *Europhys. Lett.* **57** 859
[108] Bao Z, Dodabalapur A and Lovinger A J 1996 *Appl. Phys. Lett.* **69** 4108
[109] Sirringhaus H, Tessler N and Friend R H 1998 *Science* **280** 1741
[110] Park H, Park J, Lim A K L, Anderson E H, Alivisatos A P and McEuen P L 2000 *Nature* **407** 57
[111] Zhou C, Deshpande M R, Reed M A, Jones L II and Tour J M 1997 *Appl. Phys. Lett.* **71** 611
[112] Cui X D, Primak A, Zarate X, Tomfohr J, Sankey O F, Moore A L, Moore T A, Gust D, Harris G and Lindsay S M 2001 *Science* **294** 571
[113] Reed M A, Zhou C, Muller C J, Burgin T P and Tour J M 1997 *Science* **278** 252
[114] Donhauser Z J *et al* 2001 *Science* **292** 2303
[115] Donhauser Z J, Mantooth B A, Pearl T P, Kelly K F, Nanayakkara S U and Weiss P S 2002 *Japan. J. Appl. Phys.* 1 **41** 4871
[116] Ramachandran G K, Hopson T J, Rawlett A M, Nagahara L A, Primak A and Lindsay S M 2003 *Science* **300** 1413
[117] Xu B and Tao N J 2003 *Science* **301** 1221
[118] Smit R H M, Noat Y, Untiedt C, Lang N D, van Hemert M C and van Ruitenbeek J M 2002 *Nature* **419** 906
[119] Park H, Lim A K L, Alivisatos A P, Park J and McEuen P L 1999 *Appl. Phys. Lett.* **75** 301
[120] Liang W, Shores M P, Bockrath M, Long J R and Park H 2002 *Nature* **417** 725
[121] Park J, Pasupathy A N, Goldsmith J I, Chang C, Yaish Y, Petta J R, Rinkoski M, Sethna J P, Abruña H D, McEuen P L and Ralph D C 2002 *Nature* **417** 722
[122] Zhitenev N B, Meng H and Bao Z 2002 *Phys. Rev. Lett.* **88** 226801
[123] Basch H and Ratner M A 2003 *J. Chem. Phys.* **119** 11926
[124] Yoshida K, Shimomura T, Ito K and Hayakawa R 1999 *Langmuir* **15** 910
[125] Shimomura T, Akai T, Abe T and Ito K 2002 *J. Chem. Phys.* **116** 1753
[126] Cacialli F *et al* 2002 *Nat. Mater.* **1** 160
[127] Chattopadhyay D, Galeska I and Papadimitrakopoulos F 2003 *J. Am. Chem. Soc.* **125** 3370
[128] Krupke R, Hennrich F, von Löhneysen H and Kappes M M 2003 *Science* **301** 344
[129] Zheng M, Jagota A, Semke E D, Diner B A, McLean R S, Lustig S R, Richardson R E and Tassi N G 2003 *Nat. Mater.* **2** 338
[130] Zheng M *et al* 2003 *Science* **302** 1545
[131] Collins P G, Arnold M S and Avouris P 2001 *Science* **292** 706
[132] Tans S J, Devoret M H, Dai H, Thess A, Smalley R E, Geerligs L J and Dekker C 1997 *Nature* **386** 474
[133] Postma H W C, de Jonge M, Yao Z and Dekker C 2000 *Phys. Rev.* B **62** 10653
[134] Postma H W C, Teepen T, Yao Z, Grifoni M and Dekker C 2001 *Science* **293** 76
[135] Egger R and Gogolin A O 1997 *Phys. Rev. Lett.* **79** 5082
[136] Kane C, Balents L and Fisher M P A 1997 *Phys. Rev. Lett.* **79** 5086
[137] Ishii H *et al* 2003 *Nature* **426** 540
[138] Bockrath M, Cobden D H, McEuen P L, Chopra N G, Zettl A, Thess A and Smalley R E 1997 *Science* **275** 1922
[139] Yao Z, Kane C L and Dekker C 2000 *Phys. Rev. Lett.* **84** 2941
[140] Tans S J and Dekker C 2000 *Nature* **408** 834
[141] Bachtold A, Fuhrer M S, Plyasunov S, Forero M, Anderson E H, Zettl A and McEuen P L 2000 *Phys. Rev. Lett.* **84** 6082
[142] Albrecht P M and Lyding J W 2003 *Appl. Phys. Lett.* **83** 5029
[143] Soh H T, Quate C F, Morpurgo A F, Marcus C M, Kong J and Dai H 1999 *Appl. Phys. Lett.* **75** 627

[144] Teo K B K, Chhowalla M, Amaratunga G A J, Milne W I, Hasko D G, Pirio G, Legagneux P, Wyczisk F and Pribat D 2001 *Appl. Phys. Lett.* **79** 1534
[145] Dai H 2002 *Acc. Chem. Res.* **35** 1035
[146] Kleckley S, Chai G, Zhou D, Vanfleet R and Chow L 2003 *Carbon* **41** 833
[147] Strano M S, Dyke C A, Usrey M L, Barone P W, Allen M J, Shan H, Kittrell C, Hauge R H, Tour J M and Smalley R E 2003 *Science* **301** 1519
[148] Wagner R S and Ellis W C 1964 *Appl. Phys. Lett.* **4** 89
[149] Hiruma K, Yazawa M, Katsuyama T, Ogawa K, Haraguchi K, Koguchi M and Kakibayashi H 1995 *J. Appl. Phys.* **77** 447
[150] Morales A M and Lieber C M 1998 *Science* **279** 208
[151] Zhang Y F, Tang Y H, Wang N, Yu D P, Lee C S, Bello I and Lee S T 1998 *Appl. Phys. Lett.* **72** 1835
[152] Chung S W, Yu J Y and Heath J R 2000 *Appl. Phys. Lett.* **76** 2068
[153] Ma D D D, Lee C S, Au F C K, Tong S Y and Lee S T 2003 *Science* **299** 1874
[154] Wu Y, Fan R and Yang P 2002 *Nano Lett.* **2** 83
[155] Lauhon L J, Gudiksen M S, Wang D and Lieber C M 2002 *Nature* **420** 57
[156] Gudiksen M S, Lauhon L J, Wang J, Smith D C and Lieber C M 2002 *Nature* **415** 617
[157] Hu J, Ouyang M, Yang P and Lieber C M 1999 *Nature* **399** 48
[158] Kamins T I, Williams R S, Basile D P, Hesjedal T and Harris J S 2001 *J. Appl. Phys.* **89** 1008
[159] Zhang Y F, Tang Y H, Wang N, Lee C S, Bello I and Lee S T 2000 *Phys. Rev.* B **61** 4518
[160] Huang Y, Duan X, Cui Y and Lieber C M 2002 *Nano Lett.* **2** 101
[161] Björk M T, Ohlsson B J, Sass T, Persson A I, Thelander C, Magnusson M H, Deppert K, Wallenberg L R and Samuelson L 2002 *Appl. Phys. Lett.* **80** 1058
[162] Duan X, Huang Y, Cui Y, Wang J and Lieber C M 2001 *Nature* **409** 66
[163] Duan X, Huang Y, Agarwal R and Lieber C M 2003 *Nature* **421** 241
[164] Solanki R, Huo J, Freeouf J L and Miner B 2002 *Appl. Phys. Lett.* **81** 3864
[165] Tilke A T, Simmel F C, Lorenz H, Blick R H and Kotthaus J P 2003 *Phys. Rev.* B **68** 075311
[166] Zhang Y F, Liao L S, Chan W H, Lee S T, Sammynaiken R and Sham T K 2000 *Phys. Rev.* B **61** 8298
[167] Puzder A, Williamson A J, Reboredo F A and Galli G 2003 *Phys. Rev. Lett.* **91** 157405
[168] Chopra N G, Luyken R J, Cherrey K, Crespi V H, Cohen M L, Louie S G and Zettl A 1995 *Science* **269** 966
[169] Pan Z W, Dai Z R and Wang Z L 2001 *Science* **291** 1947
[170] Yang P, Yan H, Mao S, Russo R, Johnson J, Saykally R, Morris N, Pham J, He R and Choi H J 2002 *Adv. Funct. Mater.* **12** 323
[171] Huang M H, Mao S, Feick H, Yan H, Wu Y, Kind H, Weber E, Russo R and Yang P 2001 *Science* **292** 1897
[172] Remskar M, Mrzel A, Skraba Z, Jesih A, Ceh M, Demsar J, Stadelmann P, Levy F and Mihailovic D 2001 *Science* **292** 479
[173] Goldberger J, He R, Zhang Y, Lee S, Yan H, Choi H J and Yang P 2003 *Nature* **422** 599
[174] Wang X, Sin X, Yu D, Zou B and Li Y 2003 *Adv. Mater.* **15** 1442
[175] Goringe C M, Bowler D R and Hernández E 1997 *Rep. Prog. Phys.* **60** 1447
[176] Payne M C, Teter M P, Allan D C, Arias T A and Joannopoulos J D 1992 *Rev. Mod. Phys.* **64** 1045
[177] Goedecker S 1999 *Rev. Mod. Phys.* **71** 1085
[178] Bowler D R, Miyazaki T and Gillan M J 2002 *J. Phys.: Condens. Matter* **14** 2781
[179] Soler J M, Artacho E, Gale J D, García A, Junquera J, Ordejón P and Sánchez-Portal D 2002 *J. Phys.: Condens. Matter* **14** 2745
[180] Onida G, Reining L and Rubio A 2002 *Rev. Mod. Phys.* **74** 601
[181] Anisimov V I, Aryasetiawan F and Lichtenstein A I 1997 *J. Phys.: Condens. Matter* **9** 767
[182] Georges A, Kotliar G, Krauth W and Rozenberg M J 1996 *Rev. Mod. Phys.* **68** 13
[183] Foulkes W M C, Mitas L, Needs R J and Rajagopal G 2001 *Rev. Mod. Phys.* **73** 33
[184] Yang Z, Tackett A and Ventra M D 2002 *Phys. Rev.* B **66** 041405(R)
[185] Landauer R 1957 *IBM J. Res. Dev.* **1** 223
[186] Landauer R 1996 *J. Math. Phys.* **37** 5259
[187] Imry Y and Landauer R 1999 *Rev. Mod. Phys.* **71** S306
[188] Büttiker M, Imry Y, Landauer R and Pinhas S 1985 *Phys. Rev.* B **31** 6207
[189] Fisher D S and Lee P A 1981 *Phys. Rev.* B **23** 6851
[190] Anderson P W, Thouless D J, Abrahams E and Fisher D S 1980 *Phys. Rev.* B **22** 3519
[191] Meir Y and Wingreen N S 1992 *Phys. Rev. Lett.* **68** 2512
[192] Landauer R 1989 *J. Phys.: Condens. Matter* **1** 8099
[193] Payne M C 1989 *J. Phys.: Condens. Matter* **1** 4931
[194] Büttiker M 1986 *Phys. Rev. Lett.* **57** 1761

[195] Datta S 1995 *Electronic Transport in Mesoscopic Systems* (New York: Cambridge University Press)
[196] Caroli C, Combescot R, Nozieres P and Saint-James D 1971 *J. Phys. C: Solid State Phys.* **4** 916
[197] Pendry J B, Prêtre A B and Krutzen B C H 1991 *J. Phys.: Condens. Matter* **3** 4313
[198] Todorov T N, Briggs G A D and Sutton A P 1993 *J. Phys.: Condens. Matter* **5** 2389
[199] Todorov T N 2002 *J. Phys.: Condens. Matter* **14** 3049
[200] Wang B, Wang J and Guo H 1999 *Phys. Rev. Lett.* **82** 398
[201] Wang B, Wang J and Guo H 1999 *J. Appl. Phys.* **86** 5094
[202] Taylor J, Guo H and Wang J 2001 *Phys. Rev.* B **63** 245407
[203] Lang N 1995 *Phys. Rev.* B **52** 5335
[204] Di Ventra M, Pantelides S T and Lang N D 2000 *Phys. Rev. Lett.* **84** 979
[205] Baer R and Neuhauser D 2003 *Chem. Phys. Lett.* **374** 459
[206] Kosov D S 2003 *J. Chem. Phys.* **119** 1
[207] Di Ventra M and Lang N D 2001 *Phys. Rev.* B **65** 045402
[208] Bratkovsky A M, Sutton A P and Todorov T N 1995 *Phys. Rev.* B **52** 5036
[209] Chen Y C, Zwolak M and Ventra M D 2003 *Nano Lett.* **3** 1691
[210] Samanta M P, Tian W, Datta S, Henderson J I and Kubiak C P 1996 *Phys. Rev.* B **53** R7626
[211] Sanvito S, Lambert C J, Jefferson J H and Bratkovsky A M 1999 *Phys. Rev.* B **59** 11936
[212] Yaliraki S N and Ratner M A 1999 *J. Chem. Phys.* **109** 5036
[213] Mujica V, Kemp M and Ratner M 1994 *J. Chem. Phys.* **101** 6849
[214] Sirvent C, Rodrigo J G, Vieira S, Jurczyszyn L, Mingo N and Flores F 1996 *Phys. Rev.* B **53** 16086
[215] Nardelli M B 1999 *Phys. Rev.* B **60** 7828
[216] Emberly E G and Kirczenow G 2000 *Phys. Rev.* B **62** 10451
[217] Emberly E G and Kirczenow G 2001 *Phys. Rev.* B **64** 125318
[218] Mujica V, Roitberg A E and Ratner M 2000 *J. Chem. Phys.* **112** 6834
[219] Tian W, Datta S, Hong S, Reifenberger R, Henderson J I and Kubiak C P 1998 *J. Chem. Phys.* **109** 2874
[220] Ness H and Fisher A J 1997 *Phys. Rev.* B **56** 12469
[221] Damle P S, Ghosh A W and Datta S 2001 *Phys. Rev.* B **64** 201403
[222] Palacios J J, Pérez-Jiménez A J, Louis E and Vergés J A 2001 *Phys. Rev.* B **64** 115411
[223] Nardelli M B, Fattebert J L and Bernholc J 2002 *Phys. Rev.* B **64** 245423
[224] Wortmann D, Ishida H and Blügel S 1966 *Phys. Rev.* B **66** 075113
[225] Calzolari A, Marzari N, Souza I and Nardelli M B 2004 *Phys. Rev.* B **69** 035108
[226] Di Ventra M and Pantelides S T 2000 *Phys. Rev.* B **61** 16207
[227] Todorov T N 2001 *J. Phys.: Condens. Matter* **13** 10125
[228] Todorov T N, Hoekstra J and Sutton A P 2000 *Phil. Mag.* B **80** 421
[229] Ness H and Fisher A J 1999 *Phys. Rev. Lett.* **83** 452
[230] Bowler D R and Fisher A J 2001 *Phys. Rev.* B **63** 035310
[231] Todorovic M, Fisher A J and Bowler D R 2002 *J. Phys.: Condens. Matter* **14** L749
[232] Jauho A P, Wingreen N S and Meir Y 1994 *Phys. Rev.* B **50** 5528
[233] Horsfield A P, Bowler D R and Fisher A J 2004 *J. Phys.: Condens. Matter* **16** L65
[234] Baer R and Gould R 2001 *J. Chem. Phys.* **114** 3385
[235] Baer R and Neuhauser D 2003 *Int. J. Quantum Chem.* **91** 524
[236] Nakano A, Vashishta P and Kalia R K 1991 *Phys. Rev.* B **43** 9066
[237] Todorov T N 1998 *Phil. Mag.* B **77** 965
[238] Montgomery M J, Todorov T N and Sutton A P 2002 *J. Phys.: Condens. Matter* **14** 5377
[239] Montgomery M J, Hoekstra J, Todorov T N and Sutton A P 2003 *J. Phys.: Condens. Matter* **15** 731
[240] Montgomery M J and Todorov T N 2003 *J. Phys.: Condens. Matter* **15** 8781
[241] Agraït N, Untiedt C, Rubio-Bollinger G and Vieira S 2002 *Chem. Phys.* **281** 231
[242] Caroli C, Combescot R, Nozieres P and Saint-James D 1972 *J. Phys. C: Solid State Phys.* **5** 21
[243] Bonča J and Trugman S A 1995 *Phys. Rev. Lett.* **75** 2566
[244] Bonča J and Trugman S A 1997 *Phys. Rev. Lett.* **79** 4874
[245] Bonča J, Trugman S A and Batistić I 1999 *Phys. Rev.* B **60** 1633
[246] Kornilovitch P E and Pike E R 1997 *Phys. Rev.* B **55** R8634
[247] Jeckelmann E and White S R 1998 *Phys. Rev.* B **57** 6376
[248] Romero A H, Brown D W and Lindenberg K 1998 *J. Chem. Phys.* **109** 6540
[249] Dash L K and Fisher A J 2001 *J. Phys.: Condens. Matter* **13** 5035
[250] Yanson A I, Bollinger G R, van den Brom H E, Agraït N and van Ruitenbeek J M 1998 *Nature* **395** 783
[251] Gillingham D M, Linington I and Bland J A C 2002 *J. Phys.: Condens. Matter* **14** L567
[252] Kizuka T 1998 *Phys. Rev. Lett.* **81** 4448

[253] Rego L G C, Rocha A R, Rodrigues V and Ugarte D 2003 *Phys. Rev.* B **67** 045412
[254] Nakamura A, Brandbyge M, Hansen L B and Jacobsen K W 1999 *Phys. Rev. Lett.* **82** 1538
[255] Jelínek P, Pérez R, Ortega J and Flores F 2003 *Phys. Rev.* B **68** 085403
[256] da Silva E Z, da Silva A J R and Fazzio A 2001 *Phys. Rev. Lett.* **87** 256102
[257] Sánchez-Portal D, Artacho E, Junquera J, Ordejón P, García A and Soler J M 1999 *Phys. Rev. Lett.* **83** 3884
[258] Takai Y, Kawasaki T, Kimura Y, Ikuta T and Shimizu R 2001 *Phys. Rev. Lett.* **87** 106105
[259] Koizumi H, Oshima Y, Kondo Y and Takayanagi K 2001 *Ultramicroscopy* **88** 17
[260] Novaes F D, da Silva A J R, da Silva E Z and Fazzio A 2003 *Phys. Rev. Lett.* **90** 036101
[261] Legoas S B, Galvão D S, Rodrigues V and Ugarte D 2002 *Phys. Rev. Lett.* **88** 076105
[262] Bahn S R, Lopez N, Nørskov J K and Jacobsen K W 2002 *Phys. Rev.* B **66** 081405
[263] Ribeiro F J and Cohen M L 2003 *Phys. Rev.* B **68** 035423
[264] Rubio-Bollinger G, Bahn S R, Agraït N, Jacobsen K and Vieira S 2001 *Phys. Rev. Lett.* **87** 026101
[265] Torres J, Tosatti E, Corso A D, Ercolessi F, Kohanoff J, Tolla F D and Soler J 1999 *Surf. Sci.* **426** L441
[266] da Silva E Z, Novaes F D, da Silva A J R and Fazzio A 2004 *Phys. Rev.* B **69** 115411
[267] Todorov T N, Hoekstra J and Sutton A P 2001 *Phys. Rev. Lett.* **86** 3606
[268] Wallis T M, Nilius N and Ho W 2002 *Phys. Rev. Lett.* **89** 236802
[269] Nilius N, Wallis T M and Ho W 2002 *Science* **297** 1853
[270] Nilius N, Wallis T M, Persson M and Ho W 2003 *Phys. Rev. Lett.* **90** 196103
[271] Fölsch S, Hyldgaard P, Koch R and Ploog K H 2004 *Phys. Rev. Lett.* **92** 056803
[272] Yaliraki S N, Roitberg A E, Gonzalez C, Mujica V and Ratner M A 1999 *J. Chem. Phys.* **111** 6997
[273] Emberly E G and Kirczenow G 2001 *Phys. Rev.* B **64** 235412
[274] Di Ventra M, Pantelides S T and Lang N D 2002 *Phys. Rev. Lett.* **88** 046801
[275] Lang N D and Avouris P 2001 *Phys. Rev.* B **64** 125323
[276] Di Ventra M, Kim S G, Pantelides S T and Lang N D 2001 *Phys. Rev. Lett.* **86** 288
[277] Taylor J, Brandbyge M and Stokbro K 2002 *Phys. Rev. Lett.* **89** 138301
[278] Kaun C C, Larade B and Guo H 2003 *Phys. Rev.* B **67** 121411(R)
[279] Kornilovitch P E and Bratkovsky A M 2001 *Phys. Rev.* B **64** 195413
[280] Bratkovsky A M and Kornilovitch P E 2003 *Phys. Rev.* B **67** 115307
[281] Toerker M, Fritz T, Proehl H, Gutierrez R, Grossmann F and Schmidt R 2002 *Phys. Rev.* B **65** 245422
[282] Krüger D, Fuchs H, Rousseau R, Marx D and Parrinello M 2002 *Phys. Rev. Lett.* **89** 186402
[283] Nazin G V, Qiu X H and Ho W 2003 *Science* **302** 77
[284] Joachim C, Gimzewski J K and Aviram A 2000 *Nature* **408** 541
[285] Metzger R M *et al* 1997 *J. Am. Chem. Soc.* **119** 10455
[286] Chen J, Reed M A, Rawlett A M and Tour J M 1999 *Science* **286** 1550
[287] Reed M A, Chen J, Rawlett A M, Price D W and Tour J M 2001 *Appl. Phys. Lett.* **78** 3735
[288] Liu Z, Yasseri A A, Lindsey J S and Bocian D F 2003 *Science* **302** 1543
[289] Avouris P 2002 *Acc. Chem. Res.* **35** 1026
[290] Avouris P 2002 *Chem. Phys.* **281** 429
[291] Cui Y and Lieber C M 2001 *Science* **291** 851
[292] Martel R, Schmidt T, Shea H R, Hertel T and Avouris P 1998 *Appl. Phys. Lett.* **73** 2447
[293] Tans S J, Verschueren A R M and Dekker C 1998 *Nature* **393** 49
[294] Liu X, Lee C, Zhou C and Han J 2001 *Appl. Phys. Lett.* **79** 3329
[295] Wind S J, Appenzeller J, Martel R, Derycke V and Avouris P 2002 *Appl. Phys. Lett.* **80** 3817
[296] Derycke V, Martel R, Appenzeller J and Avouris P 2002 *Appl. Phys. Lett.* **80** 2773
[297] Zhong Z, Wang D, Cui Y, Bockrath M W and Lieber C M 2003 *Science* **302** 1377
[298] Misewich J A, Martel R, Avouris P, Tsang J C, Heinze S and Tersoff J 2003 *Science* **300** 783
[299] Keren K, Berman R S, Buchstab E and Braun U S E 2003 *Science* **302** 1380
[300] Thelander C, Martensson T, Björk M T, Ohlsson B J, Larsson M W, Wallenberg L R and Samuelson L 2003 *Appl. Phys. Lett.* **83** 2052
[301] Rueckes T, Kim K, Joselevich E, Tseng G Y, Cheung C L and Lieber C M 2000 *Science* **289** 94
[302] Datta S and Das B 1990 *Appl. Phys. Lett.* **56** 665
[303] Gregg J *et al* 1997 *J. Magn. Magn. Mater.* **175** 1
[304] Prinz G A 1998 *Science* **282** 1660
[305] Wolf S A, Awschalom D D, Buhrman R A, Daughton J M, von Molnár S, Roukes M L, Chtchelkanova A Y and Treger D M 2001 *Science* **294** 1488
[306] Gregg J F, Petej I, Jouguelet E and Dennis C 2002 *J. Phys. D: Appl. Phys.* **35** R121
[307] Das Sarma S, Hwang E and Kaminski A 2003 *Solid State Commun.* **127** 99
[308] Žutić I, Fabian J and Das Sarma S 2004 *Rev. Mod. Phys.* **76** 323

[309] Pearton S J *et al* 2004 *J. Phys.: Condens. Matter* **16** R209
[310] Kelly D, Wegrowe J E, Truong T K, Hoffer X and Ansermet J P 2003 *Phys. Rev.* B **68** 134425
[311] Yamanouchi M, Chiba D, Matsukura F and Ohno H 2004 *Nature* **428** 539
[312] Sham L J 1999 *J. Magn. Magn. Mater.* **200** 219
[313] Bena C and Balents L 2002 *Phys. Rev.* B **65** 115108
[314] Emberly E G and Kirczenow G 2002 *Chem. Phys.* **281** 311
[315] Zwolak M and Di Ventra M 2002 *Appl. Phys. Lett.* **81** 925
[316] Ouyang M and Awschalom D D 2003 *Science* **301** 1074
[317] Tsukagoshi K, Alphenaar B W and Ago H 1999 *Nature* **401** 572
[318] Alphenaar B W, Tsukagoshi K and Wagner M 2001 *J. Appl. Phys.* **89** 6863
[319] Zhao B, Mönch I, Vinzelberg H, Mühl T and Schneider C M 2002 *Appl. Phys. Lett.* **80** 3144
[320] Mehrez H, Taylor J, Guo H, Wang J and Roland C 2000 *Phys. Rev. Lett.* **84** 2682
[321] Heinze S, Bode M, Kubetzka A, Pietzsch O, Nie X, Blügel S and Wiesendanger R 2000 *Science* **288** 1805
[322] Heeger A J, Kivelson S, Schrieffer J R and Su W P 1988 *Rev. Mod. Phys.* **60** 781
[323] Stoneham A M, Ramos M M D, Almeida A M, Correia H M G, Ribeiro R M, Ness H and Fisher A J 2002 *J. Phys.: Condens. Matter* **14** 9877
[324] Agraït N, Untiedt C, Rubio-Bollinger G and Vieira S 2002 *Phys. Rev. Lett.* **88** 216803
[325] Bird C F, Fisher A J and Bowler D R 2003 *Phys. Rev.* B **68** 115318
[326] Grayson M, Tsui D, Pfeiffer L N, West K and Chang A M 2001 *Phys. Rev. Lett.* **86** 2645
[327] Hilke M, Tsui D C, Grayson M, Pfeiffer L N and West K 2001 *Phys. Rev. Lett.* **87** 186806
[328] Chang A M 2003 *Rev. Mod. Phys.* **75** 1449
[329] Voit J 1994 *Rep. Prog. Phys.* **57** 977
[330] Pustilnik M and Glazman L 2004 *J. Phys.: Condens. Matter* **16** R513
[331] Smith P A, Nordquist C D, Jackson T N, Mayera T S, Martin B R, Mbindyo J and Mallouk T E 2000 *Appl. Phys. Lett.* **77** 1399
[332] Huang Y, Duan X, Wei W and Lieber C M 2001 *Science* **291** 630
[333] Melosh N A, Boukai A, Diana F, Gerardot B, Badolato A, Petroff P M and Heath J R 2003 *Science* **300** 112
[334] Yan H, Park S H, Finkelstein G, Reif J H and LaBean T H 2003 *Science* **301** 1882
[335] Hong B H, Bae S C, Lee C W, Jeong S and Kim K S 2001 *Science* **294** 348
[336] Suh S B, Hong B H, Tarakeshwar P, Youn S J, Jeong S and Kim K S 2003 *Phys. Rev.* B **67** 241402(R)
[337] Smith B W, Monthioux M and Luzzi D E 1998 *Nature* **396** 323
[338] Mickelson W, Aloni S, Han W Q, Cumings J and Zettl A 2003 *Science* **300** 467
[339] Takenobu T, Takano T, Shiraishi M, Murakami Y, Ata M, Kataura H, Achiba Y and Iwasa Y 2003 *Nat. Mater.* **2** 683
[340] McIntosh G C, Tománek D and Park Y W 2003 *Phys. Rev.* B **67** 125419
[341] Sloan J, Kirkland A I, Hutchison J L and Green M L H 2002 *Acc. Chem. Res.* **35** 1054
[342] O'Brien J L, Schofield S R, Simmons M Y, Clark R G, Dzurak A S, Curson N J, Kane B E, McAlpine N S, Hawley M E and Brown G W 2001 *Phys. Rev.* B **64** 161401
[343] Heath J R, Kuekes P J, Snider G S and Williams R S 1998 *Science* **280** 1716
[344] Stoneham A M, Fisher A J and Greenland P T 2003 *J. Phys.: Condens. Matter* **15** L447